ANALYSIS OF TIME FILTERS IN MULTISTEP METHODS

by

Nicholas Hurl

Bachelor of Mathematics, Kent State University, 2008

Submitted to the Graduate Faculty of

the Kenneth P. Dietrich School of Arts and Sciences in partial

fulfillment

of the requirements for the degree of

Doctor of Philosophy in Mathematics

University of Pittsburgh

2017

UNIVERSITY OF PITTSBURGH

KENNETH P. DIETRICH SCHOOL OF ARTS AND SCIENCES

This dissertation was presented

by

Nicholas Hurl

It was defended on

September 9th 2016

and approved by

William Layton, Professor, Department of Mathematics, University of Pittsburgh

Catalin Trenchea, Associate Professor, Department of Mathematics, University of Pittsburgh

Huiqiang Jiang, Associate Professor, Department of Mathematics, University of Pittsburgh

Patrick Smolinski, Associate Professor, Department of Mechanical Engineering and Materials Science

Dissertation Director: William Layton, Professor, Department of Mathematics, University of Pittsburgh

ABSTRACT

ANALYSIS OF TIME FILTERS IN MULTISTEP METHODS

Nicholas Hurl, PhD

University of Pittsburgh, 2017

Geophysical flow simulations have evolved sophisticated implicit-explicit time stepping methods (based on fast-slow wave splittings) followed by time filters to control any unstable models that result. Time filters are modular and parallel. Their effect on stability of the overall process has been tested in numerous simulations, but never analyzed. Stability is proven herein for the Crank-Nicolson Leapfrog (CNLF) method with the Robert-Asselin (RA) time filter and for the Crank-Nicolson Leapfrog method with the Robert-Asselin-Williams (RAW) time filter for systems by energy methods. We derive an equivalent multistep method for CNLF+RA and CNLF+RAW and stability regions are obtained. The time step restriction for energy stability of CNLF+RA is smaller than CNLF and CNLF+RAW time step restriction is even smaller. Numerical tests find that RA and RAW add numerical dissipation.

This thesis also shows that all modes of the Crank-Nicolson Leap Frog (CNLF) method are asymptotically stable under the standard timestep condition.

TABLE OF CONTENTS

LIST OF FIGURES

1.0 INTRODUCTION

The primary method for time discretization in present-day geophysical fluid dynamics (GFD) codes is the implicit-explicit (IMEX) combination Crank-Nicolson Leapfrog (CNLF) method with time filters. The advantage of CNLF is its ability to separate the fast, low energy waves into the implicit Crank-Nicolson (CN) method and the slow, high energy waves into the explicit Leapfrog method (LF). Without a time filter CNLF is stable under the same time restriction as LF, but shows a weak instability. The unstable mode of LF is credited with causing the weak instability in CNLF, that is CN is believed to not control the unstable mode of LF. The stability of different modes of CNLF is discussed in chapter 4 .

To control the weak instablity of CNLF modular time filters have been developed in geophysics community for use in combination with CNLF. The most common are the Robert-Asselin (RA) time filter and Williams' addition to RA the Robert-Asselin-Williams (RAW) time filter. The scheme consists of one step of CNLF, followed by one step of RA, followed by one step of RAW, which is Williams addition to the filter. The RA step adds numerical diffusion by reducing the curvature of the solution to stabilize the method, but reduces accuracy. The RAW step introduces some anti-diffusion to restore some lost accuarcy. Williams [W09] lists 25 major GFD codes using this approach including the Community Climate Systems Model, e.g., [TL05].

Given $N \times N$ matrices A, Λ, we consider the system for $u : [0, \infty) \to \mathbb{R}^N$

$$\begin{aligned} \frac{du}{dt} + Au &= -\Lambda u, \;\; u(0) = u^0, \text{ where} \\ A + A^T &\geq 0, \text{ and } \Lambda = -\Lambda^T. \end{aligned} \tag{1.1}$$

When $A + A^T = 0$ so $A = -A^T$ the system is exactly conservative for the euclidean norm: $|u(t)| = |u(0)|$. When $A + A^T > 0$ it is dissipative, $|u(t)| \to 0$ as $t \to \infty$.

The CNLF method followed by the Robert–Asselin–Williams (RAW) filter [AKW11, W09, W11] is as follows. Given timestep Δt and starting values u^0, v^1 (of sufficient accuracy, [V09]), find u^n, w^{n+1}, v^{n+1} satisfying

$$\text{(\textbf{CNLF} step)} \qquad \frac{w^{n+1}-u^{n-1}}{2\Delta t} = -A\frac{w^{n+1}+u^{n-1}}{2} - \Lambda v^n, \tag{1.2}$$

$$\text{(\textbf{RA} step)} \qquad u^n = v^n + \frac{\nu\alpha}{2}(w^{n+1} - 2v^n + u^{n-1}), \tag{1.3}$$

$$\text{(\textbf{W} step)} \qquad v^{n+1} = w^{n+1} + \frac{\nu(\alpha-1)}{2}(w^{n+1} - 2v^n + u^{n-1}). \tag{1.4}$$

The parameter ν is the RA filter parameter, usually $\mathcal{O}(0.01 - 0.2)$, and α is the Williams filter parameter, usually around $1/2$. If $\alpha = 1$ then the W filter step drops out and the method reduces to the CNLF method with the RA filter, which is analyzed in chapter 2 which is based on a paper [H12]. When $\alpha \neq 1$ we get an active W step, which is analyzed in chapter 3, which is based on a paper [HLLT13]. If $\nu = 0$, the unfiltered CNLF scheme is recovered.[1]

A crucial step in understanding behavior of non-commuting systems over long time calculations is the energy stability analysis. CNLF was first anlyzed by Fourier methods for scalar test problem, $y' + ay + i\lambda y = 0$ in 1963 [JK63], which led to the timestep condition necessary for stability,

$$\triangle t|\Lambda| < 1, \quad |\cdot| = \text{euclidean norm}. \tag{1.5}$$

The energy stability for systems of CNLF was proven in 2011 [LT12] showing the condition (1.5) is also sufficient. Stability of CNLF with time filters has been analyzed by root condition methods for linear constant coefficient, scalar test problems as well [R69, A72, W11, JW11]. Despite time filters adding stabilityty in many cases there are reports in which CNLf plus time filters destabilizes the method when CNLF alone is stable [JW11, RL97, DC86]. In chapters 2 and 3 the energy stability analysis of CNLF+RA and CNLF+RAW for non-commuting systems is presented complementing previous analysis and numerical tests found in [D10, W09].

In chapter 4, which is based on the paper [HLLM13], we prove (asymptotic) stability of the so-called *unstable mode* (or *computational mode*) of the CNLF method applied to (1.1).

[1] In chapters 2 and 3 we assume $\nu \in (0, 1]$ throughout. In chapter 4 $\nu = 0$ since we focus on CNLF alone.

The solution to (1.1) under the conditions prescribed satisfies $u(t) \to 0$ as $t \to \infty$ so any growth in the approximate solution is a numerics induced instability. The CNLF method is the $\nu = 0$ case from above: given u^0, u^1, for $n \geq 2$

$$\frac{u^{n+1} - u^{n-1}}{2\triangle t} + A\frac{u^{n+1} + u^{n-1}}{2} + \Lambda u^n = 0. \tag{CNLF}$$

It is often reported that as $n \to \infty$

$$\begin{aligned} &\text{Stable Mode: } |u^{n+1} + u^{n-1}| \to 0, \\ &\text{Unstable Mode: } |u^{n+1} - u^{n-1}| \to \infty. \end{aligned} \tag{1.6}$$

One mystery is that since CNLF is stable under (1.5), no growth is possible in linear theory and yet time filters to deal with (1.6) are nearly universal in practice, [JW11]. It is an open question to determine if this could be due to a gap for IMEX methods (e.g., [ARW95], [CM10], [FHV96], [HV03], [V80], [V09]) between necessary conditions from root condition analysis and sufficient ones for systems, to accumulation in the unstable mode of roundoff errors, to imperfect imposition of the timestep condition, to nonlinearities [D10] or other unknown causes. We prove that under (1.5) *the CNLF unstable mode is (asymptotically) stable*. This result, consistent with numerical tests in Section 4.3, supports the scenario that growth in the unstable mode is due to imperfect imposition of and thus slight violation of (1.5) or due to nonlinerity.

2.0 ENERGY STABILITY ANALYSIS OF CRANK-NICOLSON-LEAPFROG METHOD WITH THE ROBERT-ASSELIN FILTER

2.1 INTRODUCTION

The most common method for timestepping in atmosphere, ocean and climate models is the implicit-explicit combination of the Crank-Nicolson-Leapfrog (CNLF) method because it allows separate treatment of the fast, low energy wave from the slow, high energy ones, e.g. Kalnay [K03], Durran [D10], Robert [R69], Asselin [A72], Williams [W11], Thomas and Loft [TL05]. For example Williams [W09] gives a list of 16 atmosphere, ocean and climate codes based on CNLF plus time filters. CNLF has a weak instability usually attributed to CN not damping the unstable mode of Leapfrog [D10, GS98, F73, V09]. Thus sophisticated tools based on modular time filters have been developed in the geophysics community for use in combination with CNLF. The most popular are the Robert-Asselin (RA) filter [R69, A72], see (2.4) below, and Williams' addition to the RA filter the RAW filter [AKW11, W09, W11]. We study herein the combination CNLF+RA.

In spite of its wide use and attention, there has been no stability analysis of CNLF + RA for (non-commuting) systems by energy methods, a step which is critical to understand its use in nonlinear systems and for large time calculations. CNLF was first analyzed for scalar problems in 1963 [JK63] by Fourier methods and its stability for systems in 2012 [LT12]. Stability of CNLF+RA has been analyzed by root condition methods (for linear constant coefficient, scalar test problems) [R69, A72, W11, JW11]. However, there have also been cases reported [JW11, RL97, DC86] of CNLF + time filters destabilizing a simulation in which CNLF alone is stable. This issue also is addressed herein.

The first energy analysis of stability of CNLF+RA time filter for systems will be presented

in this chapter. To begin, consider the initial value problem:

$$\begin{cases} u'(t) + Au(t) + \Lambda u(t) = 0 & \text{for } t > 0 \\ u(0) = u_0 \end{cases} \tag{2.1}$$

where $u : [0, \infty) \to \mathbb{R}^N$, and A, Λ are NxN real matrices with

$$\begin{cases} A = A^T > 0 \\ \Lambda = -\Lambda^T \end{cases} \tag{2.2}$$

An equation with this form arises in spatial discretizations of linearized flow problems with Coriolis forces and for Stokes-Darcy problem.

Let Δt be the time step and $u^n \approx u(t^n)$ for $t^n = n\Delta t$. Here ν is a parameter, usually small (e.g. $\nu \sim 10^{-1}$) and recomend by [A72] to satisfy $0 < \nu < 1$. The usual CNLF+RA time filter method for (2.1) is: given u^{n-1}, v^n find u^n, v^{n+1} satisfying

$$\frac{v^{n+1} - u^{n-1}}{2\Delta t} + A(\frac{v^{n+1} + u^{n-1}}{2}) + \Lambda(v^n) = 0, \tag{2.3}$$

$$u^n = v^n + \frac{\nu}{2}(v^{n+1} - 2v^n + u^{n-1}) \tag{2.4}$$

The step (2.3) is CNLF and (2.4) is the RA time filter. Here v^n denotes an unfiltered transitional value and u^n the filtered solution. In the preliminary section 2.2 we recall the motivation for the RA filter and collect in Proposition 1 the results in [R69, A72, K03] that RA reduces the discrete curvature (precisely defined). In Section 2.3 the intermediate values v^n, v^{n+1} can be eliminated from (2.3) and (2.4), reducing CNLF+RA to a non-standard linear multistep method (LMM). We prove:

Theorem 1. *The approximation v^n and u^n from CNLF+RA, (2.3) (2.4), both satisfy*

$$u^{n+1} - \nu u^n - (1-\nu)u^{n-1} + \Delta t A\left(u^{n+1} + (1-\nu)u^{n-1}\right) + 2\Delta t \Lambda(u^n - \frac{\nu}{2}u^{n-1}) = 0 \tag{2.5}$$

for $n \geq 2$.

Next, we give in section 2.3 an energy method proof of stability- the main result of this work. The proof delineates the discrete system energy and the method-induced numerical dissipation.

The usual Euclidean inner product and norm are $(u, v) = v^T u$ and $\|u\|^2 = (u, u)$. The A-norm $\|u\|_A^2 := (Au, u)$ and the induced euclidean matrix norm, $\|\Lambda\| = \sqrt{\lambda_{max}(\Lambda^T \Lambda)}$ will be utilized later. Define the system energy and numerical dissipation of CNLF+RA as:

$$E^{n+1/2} := (1 - \frac{\nu}{2})\Big[\|u^{n+1}\|^2 + (1 - \nu)\|u^n\|^2 + 2(\Delta t \Lambda u^n, u^{n+1})\Big]$$

and

$$D^n := \frac{\nu}{2}\|\Delta t \Lambda(u^n - u^{n-1}) + u^{n+1} - u^n\|^2 + \frac{\nu(1-\nu)}{2}\|u^n - u^{n-1}\|^2 - \frac{\nu}{2}\|\Delta t \Lambda(u^n - u^{n-1})\|^2.$$

We prove:

Theorem 2. *Consider (2.3) and (2.4). If the parameter ν satisfies*

$$0 < \nu < 1 - (\|\Lambda\|\Delta t)^2$$

or equivalently

$$\Delta t\|\Lambda\| < \sqrt{1 - \nu} < 1$$

then $\|u^N\|$ remains bounded and in fact $\|u^N\| \to 0$ as $t^N \to \infty$. In particular for $N \geq 1$, $D^N \geq 0$ and

$$E^{N+1/2} + \sum_{n=1}^{N} \Delta t\|u^{n+1} + (1 - \nu)u^{n-1})\|_A^2 + \sum_{n=1}^{N} D^n = E^{1/2}.$$

Remark 1. *If A is positive semidefinite energy stability still holds, but not necessarily energy dissipation.*

Let us denote the maximum energy stable timestep proven for CNLF and CNLF+RA as, respectively, Δt_{CNLF} and Δt_{RA}. Previously it has been shown [LT12] that $\Delta t_{CNLF} = \frac{1}{\|\Lambda\|}$ and Theorem 2 has showed us $\Delta t_{RA} = \frac{\sqrt{1-\nu}}{\|\Lambda\|}$ (Though Δt_{RA} may be improvable). We find that the two quantities have the relationship

$$\Delta t_{RA} = \sqrt{1-\nu}\Delta t_{CNLF}.$$

Though the time step restriction for CNLF+RA is smaller than CNLF, CNLF+RA dissipates nonphysical energy in the unstable mode of CNLF, explaining its necessity in GFD calculations.

Stability regions of CNLF+RA are derived in section 2.4 for representive values of ν. The scheme (2.5) fits the form of a Implicit-Explicit (IMEX) method in which stability and convergence results have been study [C80, ARW95, FHV96, HR07]. The stability of the combined IMEX method is not guaranteed by the stability of the individual implicit and explicit methods [FHV96]. The scalar test equation used to study linear stability of IMEX methods is

$$u_t + au + \lambda u = 0 \tag{2.6}$$

where a corresponds to an eigenvalue of A (hence a is real), λ corresponds to an eigenvalue of Λ (hence λ is purely imaginary and (2.6) arises when A and Λ commute. These regions give insight into how the RA step can induce instabilities when computing near the CFL limit (possibly related to anomalies [JW11]) and why CNLF+RA is in most cases more stable than CNLF alone.

Section 2.5 presents numerical tests showing how stability is sensitive to Δt_{RA}, the time step restriction given in Theorem 2.

Remark 2. *CNLF+RA is only first order accurate while CNLF is second order [ARW95]. The RAW filter [W09] adds another filter step to CNLF+RA increasing its accuracy and reducing its numerical dissipation.*

2.2 CURVATURE EVOLUTION

The description of the RA filter in [R69, A72, W11] is that it stabilizes by reducing the discrete curvature. We summarize and quantify this property of RA in this preliminary section.

Definition 1. *The discrete curvature of ϕ^n is defined by*

$$\kappa(\phi^n) = \phi^{n+1} - 2\phi^n + \phi^{n-1}.$$

If u^n, v^n satisfy (2.3), (2.4), we denote the discrete curvatures before the RA step (2.4) by

$$\kappa^n_{CNLF} = v^{n+1} - 2v^n + u^{n-1}$$

and after the RA step by

$$\kappa^n_{RA} = v^{n+1} - 2u^n + u^{n-1}.$$

The fundamental property of RA is curvature reduction.

Proposition 1. *([R69, A72]) For every $n \geq 1$ we have*

$$\kappa^n_{RA} = (1-\nu)\kappa^n_{CNLF}.$$

Therefore for $0 < \nu < 1$, $|\kappa^n_{RA}| < |\kappa^n_{CNLF}|$, unless both are zero.

Proof. A calculation with (2.4) shows us first that

$$u^n = v^n + \frac{\nu}{2}\kappa^n_{CNLF} \tag{2.7}$$

and second that

$$\begin{aligned}\kappa^n_{RA} = v^{n+1} - 2u^n + u^{n-1} \\ &= (v^{n+1} - 2v^n + u^{n-1}) + 2(v^n - u^n) \\ &= \kappa^n_{CNLF} + 2(\frac{-\nu}{2}\kappa^n_{CNLF}) = (1-\nu)\kappa^n_{CNLF}\end{aligned}$$

□

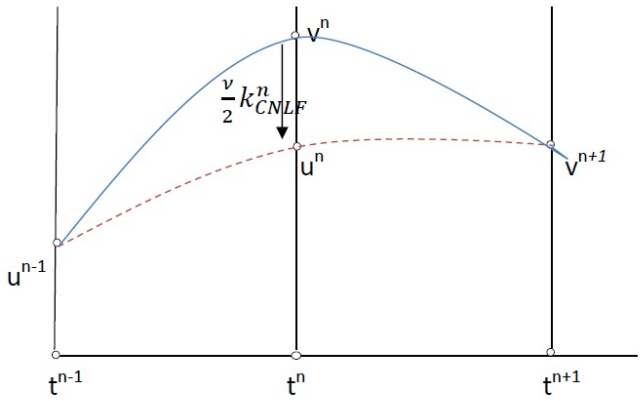

Figure 1: The energy is decreased

The simplest approach to studying stability of CNLF+RA is to check if each step reduces some system energy individually. Unfortunately, this is not true in the simplest sense. Figures 1 and 2, based on an description of time filters in [A72, W11, R69], show that RA can both decrease and increase energy. Both figures are 2d plots of solution vs time at three different times. Figure 1 presents the case when the RA step decreases the energy, and figure 2 the case of increased energy.

In both figures the solid blue curve shows the CNLF solution, the solution before the filter step is completed, and the dotted red curve shows the CNLF+RA solution. The relationship shown in (2.7) demonstrates how the filter step adjusts the CNLF solution to CNLF+RA which is illustrated in figures 1 and 2 by the arrow.

The discrete curvature of the solid blue curve in figures 1 and 2 is κ^n_{CNLF} and the dotted red line has the discrete curvature κ^n_{RA}. The figures depict how the curvature is reduced from κ^n_{RA} to κ^n_{CNLF} as predicted by Proposition 1.

We prove next that the curvature κ^n_{CNLF} and κ^n_{RA} themselves evolve according to the multistep method (2.5).

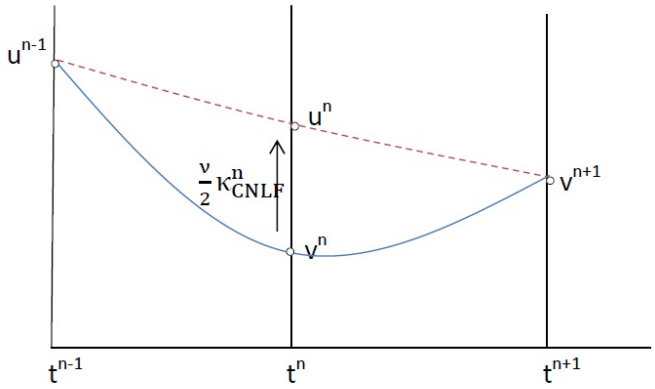

Figure 2: The energy is increased

Proposition 2. *Both κ^n_{CNLF}, and κ^n_{RA} satisfy*

$$\kappa^{n+1} - \nu\kappa^n - (1-\nu)\kappa^{n-1} + \Delta t A\left(\kappa^{n+1} + (1-\nu)\kappa^{n-1}\right) + 2\Delta t\Lambda(\kappa^n - \frac{\nu}{2}\kappa^{n-1}) = 0$$

for $n \geq 2$.

Proof. Begin with (2.3). We find from Definition 1:

$$\kappa\big(v^{n+1} - u^{n-1} + \Delta t A(v^{n+1} + u^{n-1}) + 2\Delta t\Lambda(v^n)\big) = 0$$

which by linearity implies

$$\kappa(v^{n+1}) - \kappa(u^{n-1}) + \Delta t A(\kappa(v^{n+1}) + \kappa(u^{n-1})) + 2\Delta t\Lambda(\kappa(v^n)) = 0. \tag{2.8}$$

We will make three calculations each on a part of (2.8). First consider the first two terms of (2.8). Using (2.4) we write them as a combination of κ^m_{CNLF} for $m = n+1, n, n-1$ as follows:

$$\begin{aligned}
\kappa(v^{n+1}) - \kappa(u^{n-1}) &= (v^{n+2} - 2v^{n+1} + v^n) - (u^n - 2u^{n-1} + u^{n-2}) \\
&= (v^{n+2} - 2v^{n+1} + u^n) + (v^n - u^n) \\
&\quad -[(v^n - 2v^{n-1} + u^{n-2}) + (u^n - v^n) + 2(v^{n-1} - u^{n-1})] \\
&= \kappa^{n+1}_{CNLF} + \frac{-\nu}{2}\kappa^n_{CNLF} - [\kappa^{n-1}_{CNLF} + \frac{\nu}{2}\kappa^n_{CNLF} + 2\frac{-\nu}{2}\kappa^{n-1}_{CNLF}] \\
&= \kappa^{n+1}_{CNLF} - \nu\kappa^n_{CNLF} - (1-\nu)\kappa^{n-1}_{CNLF}. \qquad (2.9)
\end{aligned}$$

Similarily we make a second calculation on the terms of (2.8) that A is operating on using (2.4) and write them as a combination of κ^m_{CNLF} for $m = n+1, n, n-1$

$$\begin{aligned}
\kappa(v^{n+1}) + \kappa(u^{n-1}) &= (v^{n+2} - 2v^{n+1} + v^n) + (u^n - 2u^{n-1} + u^{n-2}) \\
&= (v^{n+2} - 2v^{n+1} + u^n) + (v^n - u^n) \\
&\quad +[(v^n - 2v^{n-1} + u^{n-2}) + (u^n - v^n) + 2(v^{n-1} - u^{n-1})] \\
&= \kappa^{n+1}_{CNLF} + \frac{-\nu}{2}\kappa^n_{CNLF} + [\kappa^{n-1}_{CNLF} + \frac{\nu}{2}\kappa^n_{CNLF} + 2\frac{-\nu}{2}\kappa^{n-1}_{CNLF}] \\
&= \kappa^{n+1}_{CNLF} + (1-\nu)\kappa^{n-1}_{CNLF}. \qquad (2.10)
\end{aligned}$$

A third calculation is then made on the term of (2.8) that Λ is operating on using (2.4) to write it as a combination of κ^m_{CNLF} for $m = n+1, n, n-1$

$$\begin{aligned}
\kappa(v^n) = v^{n+1} - 2v^n + v^{n-1} &= (v^{n+1} - 2v^n + u^{n-1}) + (v^{n-1} - u^{n-1}) \\
&= \kappa^n_{CNLF} - \frac{\nu}{2}\kappa^{n-1}_{CNLF}. \qquad (2.11)
\end{aligned}$$

To find the result for κ^n_{CNLF} we substitute each of the three calculations (2.9), (2.10), (2.11) above for the appropriate terms of (2.8). Hence

$$\begin{aligned}
&\kappa^{n+1}_{CNLF} - \nu\kappa^n_{CNLF} - (1-\nu)\kappa^{n-1}_{CNLF} + \Delta t A(\kappa^{n+1}_{CNLF} + (1-\nu)\kappa^{n-1}_{CNLF}) \\
&\qquad + 2\Delta t\Lambda(\kappa^n_{CNLF} - \frac{\nu}{2}\kappa^{n-1}_{CNLF}) = 0. \qquad (2.12)
\end{aligned}$$

From the curvature reduction property found in proposition 1 $\kappa^n_{RA} = (1-\nu)\kappa^n_{CNLF}$. By the linearity of A and Λ multiplying through by $1-\nu$ in equation (2.12) converts all κ^m_{CNLF} to κ^m_{RA} for $m = n+1, n, n-1$ completing the result for κ^n_{RA}. □

2.3 ENERGY STABILITY

This section gives a detailed proof of energy stability. To begin we prove Theorem 1.

2.3.1 Proof of Theorem 1: CNLF+RA is a linear multistep method

Proof. The RA step, (2.4), can be rearranged to read

$$u^n - \frac{\nu}{2}u^{n-1} = \frac{\nu}{2}v^{n+1} + (1-\nu)v^n \tag{2.13}$$

Subtract CNLF at time level t^n multiplied by $\frac{\nu}{2}$ from CNLF at time level t^{n+1} (i.e (CNLF at t^{n+1})$-\frac{\nu}{2}$ (CNLF at t^n)). By linearity we obtain

$$(v^{n+2} - \frac{\nu}{2}v^{n+1}) - (u^n - \frac{\nu}{2}u^{n-1}) + \Delta t A\left(v^{n+2} - \frac{\nu}{2}v^{n+1} + u^n - \frac{\nu}{2}u^{n-1}\right) + 2\Delta t\Lambda(v^{n+1} - \frac{\nu}{2}v^n) = 0 \tag{2.14}$$

The left hand side of (2.13) appears twice in (2.14). We substitute (2.13) into (2.14) and eliminate u^n and u^{n-1} which completes the proof for v^n. Moving forward we recall that from Proposition 2, κ^n_{CNLF} also satisfies the (2.5). Since both v^n and κ^n_{CNLF} satisfy the linear multistep method (2.5), the relationship (1), $u^n = v^n + \frac{\nu}{2}\kappa^n_{CNLF}$ gives the result for u^n. □

The linear multistep method (2.5) can be rewritten as

$$\frac{u^{n+1} - u^{n-1}}{2\Delta t} + A\left(\frac{u^{n+1} + u^{n-1}}{2}\right) + \Lambda\left(u^n\right) - \frac{\nu}{2}\left(\frac{u^n - u^{n-1}}{\Delta t} + A\left(u^{n-1}\right) + \Lambda\left(u^{n-1}\right)\right) = 0. \tag{2.15}$$

The parameter ν in (2.4) scales the deviation of CNLF+RA from CNLF, and plays that role in (2.15) as well. The part of (2.15) not multiplied by ν is CNLF centered at t^n, and the part multiplied by ν is a Forward Euler step centered at t^{n-1}. Thus CNLF+RA can be thought of as CNLF with a penalty Forward Euler step at the previous time level. This shows that *the solution of CNLF+RA will differ from the solution of CNLF when u^n is not the solution of Forward Euler at t^{n-1}.*

2.3.2 Proof of Theorem 2: Energy stability

We will now prove Theorem 2 the main result of this chapter.

Proof. Take the inner product of (2.5) with $u^{n+1} + (1-\nu)u^{n-1}$. We find

$$\begin{aligned}(u^{n+1} - \nu u^n + (\nu-1)u^{n-1}, u^{n+1} + (1-\nu)u^{n-1}) \\ + \Delta t(A(u^{n+1} + (1-\nu)u^{n-1}), u^{n+1} + (1-\nu)u^{n-1}) \\ + \Delta t(\Lambda(2u^n - \nu u^{n-1}), u^{n+1} + (1-\nu)u^{n-1}) = 0\end{aligned}$$

expanding gives

$$\begin{aligned}\|u^{n+1}\|^2 + (1-\nu)(u^{n+1}, u^{n-1}) - \nu(u^n, u^{n+1}) - \nu(1-\nu)(u^n, u^{n-1}) \\ + (\nu-1)(u^{n-1}, u^{n+1}) + (\nu-1)(1-\nu)\|u^{n-1}\|^2 \\ + \Delta t\|u^{n+1} + (1-\nu)u^{n-1})\|_A^2 \\ + 2\Delta t(\Lambda u^n, u^{n+1}) + 2(1-\nu)\Delta t(\Lambda u^n, u^{n-1}) - \nu\Delta t(\Lambda u^{n-1}, u^{n+1}) = 0.\end{aligned}$$

Here we have use the skew-symmetric property $(\Lambda u^{n-1}, u^{n-1}) = 0$. Grouping like terms we find energy terms and identify a telescoping part of the Λ terms we obtain

$$\begin{aligned}\|u^{n+1}\|^2 - (1-\nu)^2\|u^{n-1}\|^2 \\ - \nu(u^{n+1}, u^n) - \nu(1-\nu)(u^n, u^{n-1}) \\ + \Delta t\|u^{n+1} + (1-\nu)u^{n-1})\|_A^2 \\ + (2-\nu)\Delta t[(\Lambda u^n, u^{n+1}) - (\Lambda u^{n-1}, u^n)] \\ + \nu\Delta t[(\Lambda u^n, u^{n+1}) + (\Lambda u^{n-1}, u^n) - (\Lambda u^{n-1}, u^{n+1})] = 0.\end{aligned}$$

Again by the skew symmetry of Λ,

$$\begin{aligned}\|u^{n+1}\|^2 - (1-\nu)^2\|u^{n-1}\|^2 \\ - \nu(u^{n+1}, u^n) - \nu(1-\nu)(u^n, u^{n-1}) \\ + \Delta t\|u^{n+1} + (1-\nu)u^{n-1})\|_A^2 \\ + (2-\nu)\Delta t[(\Lambda u^n, u^{n+1}) - (\Lambda u^{n-1}, u^n)] \\ + \nu(\Delta t\Lambda(u^n - u^{n-1}), u^{n+1} - u^n) = 0. \quad (2.16)\end{aligned}$$

Next we will use the polarization identity

$$(a,b) = -\frac{1}{2}\|a-b\|^2 + \frac{1}{2}\|a\|^2 + \frac{1}{2}\|b\|^2$$

for the inner products on the second line of (2.16) and

$$(a,b) = \frac{1}{2}\|a+b\|^2 - \frac{1}{2}\|a\|^2 - \frac{1}{2}\|b\|^2$$

for the inner product on the last line of (2.16). We obtain

$$\begin{aligned}
&\|u^{n+1}\|^2 - (1-\nu)^2\|u^{n-1}\|^2 \\
&\qquad + \frac{\nu}{2}\|u^{n+1}-u^n\|^2 - \frac{\nu}{2}\|u^{n+1}\|^2 - \frac{\nu}{2}\|u^n\|^2 \\
&\quad + \frac{\nu(1-\nu)}{2}\|u^n-u^{n-1}\|^2 - \frac{\nu(1-\nu)}{2}\|u^n\|^2 - \frac{\nu(1-\nu)}{2}\|u^{n-1}\|^2 \\
&\qquad + \Delta t\|u^{n+1}+(1-\nu)u^{n-1})\|_A^2 \\
&\qquad + (2-\nu)\Delta t[(\Lambda u^n, u^{n+1}) - (\Lambda u^{n-1}, u^n)] \\
&\quad + \frac{\nu}{2}\|\Delta t\Lambda(u^n-u^{n-1}) + u^{n+1} - u^n\|^2 - \frac{\nu}{2}\|\Delta t\Lambda(u^n-u^{n-1})\|^2 - \frac{\nu}{2}\|u^{n+1}-u^n\|^2 = 0.
\end{aligned}$$

Grouping like terms this becomes

$$\begin{aligned}
&(1-\frac{\nu}{2})\|u^{n+1}\|^2 - (\nu - \frac{\nu^2}{2})\|u^n\|^2 - (1 - \frac{3\nu}{2} + \frac{\nu^2}{2})\|u^{n-1}\|^2 \\
&\qquad + \Delta t\|u^{n+1}+(1-\nu)u^{n-1})\|_A^2 \\
&\qquad + (2-\nu)\Delta t[(\Lambda u^n, u^{n+1}) - (\Lambda u^{n-1}, u^n)] \\
&\quad + \frac{\nu(1-\nu)}{2}\|u^n-u^{n-1}\|^2 - \frac{\nu}{2}\|\Delta t\Lambda(u^n-u^{n-1})\|^2 \\
&\qquad + \frac{\nu}{2}\|\Delta t\Lambda(u^n-u^{n-1}) + u^{n+1} - u^n\|^2 = 0,
\end{aligned}$$

and rewritten as

$$\begin{aligned}
&(1-\frac{\nu}{2})\|u^{n+1}\|^2 - \nu(1-\frac{\nu}{2})\|u^n\|^2 - (1-\frac{\nu}{2})(1-\nu)\|u^{n-1}\|^2 \\
&\qquad + 2(1-\frac{\nu}{2})[(\Delta t\Lambda u^n, u^{n+1}) - (\Delta t\Lambda u^{n-1}, u^n)] \\
&\qquad + \Delta t\|u^{n+1}+(1-\nu)u^{n-1})\|_A^2 \\
&\quad + \frac{\nu(1-\nu)}{2}\|u^n-u^{n-1}\|^2 - \frac{\nu}{2}\|\Delta t\Lambda(u^n-u^{n-1})\|^2 \\
&\qquad + \frac{\nu}{2}\|\Delta t\Lambda(u^n-u^{n-1}) + u^{n+1} - u^n\|^2 = 0.
\end{aligned}$$

Define the CNLF+RA system energy as

$$E^{n+1/2} := (1-\frac{\nu}{2})\Big[\|u^{n+1}\|^2 + (1-\nu)\|u^n\|^2 + 2(\Delta t\Lambda u^n, u^{n+1})\Big].$$

The energy equality then reduces to

$$\begin{aligned} E^{n+1/2} - E^{n-1/2} + \big[&\Delta t\|u^{n+1} + (1-\nu)u^{n-1})\|_A^2 \\ &+ \frac{\nu}{2}\|\Delta t\Lambda(u^n - u^{n-1}) + u^{n+1} - u^n\|^2 \\ &+ \frac{\nu(1-\nu)}{2}\|u^n - u^{n-1}\|^2 - \frac{\nu}{2}\|\Delta t\Lambda(u^n - u^{n-1})\|^2\big] = 0. \quad (2.17) \end{aligned}$$

To go further we must prove $E^{n+1/2}$ is positive for all n and the term in (2.17) inside the brackets is non-negative (and hence a dissipation term). Since Λ is bounded operator we have

$$\begin{aligned} 2(\Delta t\Lambda u^n, u^{n+1}) &\le 2\|\Delta t\Lambda u^n\|\|u^{n+1}\| \\ &\le \|\Delta t\Lambda u^n\|^2 + \|u^{n+1}\|^2 \le (\Delta t\|\Lambda\|)^2\|u^n\|^2 + \|u^{n+1}\|^2 \end{aligned}$$

Under the assumed time step restriction $1-\nu-(\Delta t\|\Lambda\|)^2 > 0$ if $u^{n+1}, u^n \neq 0$ then

$$\begin{aligned} E^{n+1/2} &\ge (1-\frac{\nu}{2})\Big[\|u^{n+1}\|^2 + (1-\nu)\|u^n\|^2 - (\Delta t\|\Lambda\|)^2\|u^n\|^2 - \|u^{n+1}\|^2\Big] \\ &\ge (1-\frac{\nu}{2})\big[1-\nu-(\Delta t\|\Lambda\|)^2\big]\|u^n\|^2 > 0. \end{aligned}$$

Also note if $u^{n+1} = u^n = 0$ then $E^{n+1/2} = 0$. Let the CNLF+RA numerical dissipation be defined as

$$\begin{aligned} D^n := \frac{\nu}{2}&\|\Delta t\Lambda(u^n - u^{n-1}) + u^{n+1} - u^n\|^2 \\ &+ \frac{\nu(1-\nu)}{2}\|u^n - u^{n-1}\|^2 - \frac{\nu}{2}\|\Delta t\Lambda(u^n - u^{n-1})\|^2. \end{aligned}$$

We find D^n is nonnegative under the assumed time restriction

$$\begin{aligned} D^n &\ge \frac{\nu(1-\nu)}{2}\|u^n - u^{n-1}\|^2 - \frac{\nu}{2}\|\Delta t\Lambda(u^n - u^{n-1})\|^2 \\ &\ge \Big[\frac{\nu(1-\nu)}{2} - \frac{\nu}{2}(\Delta t\|\Lambda\|)^2\Big]\|u^n - u^{n-1}\|^2 \\ &\ge \frac{\nu}{2}\Big[1-\nu-(\Delta t\|\Lambda\|)^2\Big]\|u^n - u^{n-1}\|^2 \ge 0. \quad (2.18) \end{aligned}$$

Therefore continuing from (2.17)

$$E^{n+1/2} - E^{n-1/2} + \Delta t \|u^{n+1} + (1-\nu)u^{n-1})\|_A^2 + D^n = 0$$

and summing from $n = 1$ to $n = N$ we find

$$E^{N+1/2} + \sum_{n=1}^{N} \Delta t \|u^{n+1} + (1-\nu)u^{n-1})\|_A^2 + \sum_{n=1}^{N} D^n = E^{1/2}. \tag{2.19}$$

This proves stability. If u^1 and u^0 are bounded solutions of (2.1) at time level t^1 and t^0 respectively, then $E^{1/2}$ is bounded and hence $E^{N+1/2}$ and in turn $\|u^{N+1}\|$ are bounded.

Next we show $\|u^N\| \to 0$. Since the right hand side of (2.19) is independent of N, the left hand side must be uniformly bounded. Therefore (2.19) and (2.18) imply

$$\frac{\nu}{2} \sum_{n=1}^{\infty} \|u^n - u^{n-1}\|^2 < \infty \qquad \text{and} \qquad \sum_{n=1}^{\infty} \|u^{n+1} + (1-\nu)u^{n-1}\|_A^2 < \infty$$

and hence as $n \to \infty$

$$\frac{\nu}{2} \|u^n - u^{n-1}\| \to 0 \qquad \text{and} \qquad \|u^{n+1} + (1-\nu)u^{n-1}\|_A \to 0 \tag{2.20}$$

By the triangle inequality and equivalency of norms

$$\begin{aligned}(2-\nu)\|u^{n-1}\| &= \|(u^{n+1} + (1-\nu)u^{n-1}) - (u^{n+1} - u^n) - (u^n - u^{n-1})\| \\ &\leq \|u^{n+1} + (1-\nu)u^{n-1}\| + \|u^{n+1} - u^n\| + \|u^n - u^{n-1}\| \\ &\leq C\|u^{n+1} + (1-\nu)u^{n-1}\|_A + \|u^{n+1} - u^n\| + \|u^n - u^{n-1}\| \end{aligned} \tag{2.21}$$

for some constant C (depending on A). By hypothesis $0 < \nu < 1$ and hence the left hand side of (2.21) is positive and by (2.20) the right hand side of (2.21) to go to 0 as $n \to \infty$. Thus

$$\lim_{n\to\infty} \|u^n\| = 0.$$

□

Remark 3. *We observe from* (2.20) *that CNLF+RA prevents decoupling of the even and odd time steps.*

2.4 STABILITY REGIONS

In the previous section we have proven a sufficient condition on the time restriction, the filter parameter ν and the eigenvalues of Λ for energy stability. The current section will derive and plot the stability regions in which we observe the relationship of these quantities and of the eigenvalues of A. To begin we apply CNLF+RA to (2.6): Given $u^{n-1}, v^n \in X$ find $u^n, v^{n+1} \in X$ by

$$\frac{v^{n+1} - u^{n-1}}{2\Delta t} + a\frac{v^{n+1} + u^{n-1}}{2} + \lambda v^n = 0$$
$$u^n = v^n + \frac{\nu}{2}(v^{n+1} - 2v^n + u^{n-1}).$$

which by Theorem 1 evolves according to

$$u^{n+1} - \nu u^n - (1-\nu)u^{n-1} + \Delta t a\left(u^{n+1} + (1-\nu)u^{n-1}\right) + 2\Delta t\lambda(u^n - \frac{\nu}{2}u^{n-1}) = 0 \quad (2.22)$$

Define the characteristic polynomials following [HR07],

$$\rho(\zeta) := \zeta^{k+1} - \nu\zeta^k - (1-\nu)\zeta^{k-1}$$

$$\sigma(\zeta) := \zeta^{k+1} + (1-\nu)\zeta^{k-1}$$

$$\hat{\sigma}(\zeta) := 2\zeta^k - \nu\zeta^{k-1}$$

and the IMEX stablity polynomial as

$$\pi(\zeta; z, w) = \rho(\zeta) - z\sigma(\zeta) + w\hat{\sigma}(\zeta)$$

where $z = -\Delta t a$, $w = \Delta t\lambda$. A necessary condition for stability is (i) all roots of π have modulus less than or equal to one and (ii) multiple roots have modulus strictly less than one [FHV96]. The stability region of the IMEX method (2.3), (2.4) is defined to be the region in $\mathbb{C}^2$

$$S = \{(z, w) \in \mathbb{C}^2 : \pi(\zeta; z, w) = 0 \implies |\zeta| < 1\}.$$

Since we are restricting our attention in (2.6) to real a and purely imaginary λ we are more interested in the stability region

$$\bar{S} = \{(z, w) : z \in \mathbb{R}, w \text{ purely imaginary}, \pi(\zeta; z, w) = 0 \implies |\zeta| < 1\}.$$

A 2d plot will be produced z vs. w of the boundary of $\bar{S}$. We will outline the proceedure. Consider $(z_0, w_0) \in \partial\bar{S}$. At least one root of $\pi(\zeta; z_0, w_0)$ will have modulus equal to one. Denote this root as $\zeta_0 = e^{i\theta_0}$ some $\theta_0 \in [0, 2\pi)$. Now solving $\pi(e^{i\theta_0}; z_0, w_0) = 0$ for w_0 we find

$$w_0 = \frac{-\rho(e^{i\theta_0}) + z_0\sigma(e^{i\theta_0})}{\hat{\sigma}(e^{i\theta_0})}.$$

We may think of w_0 as depending on z_0 and θ_0. For each z let us consider the curve

$$\Gamma_z : \frac{-\rho(\zeta) + z\sigma(\zeta)}{\hat{\sigma}(\zeta)}, \quad \zeta = \exp(i\theta), \quad 0 \le \theta < 2\pi.$$

This curve contains all boundary points (possible more). Since w is purely imaginary for a fix z we find θ values such that Γ_z is purely imaginary, and then plot (z, Γ_z).

We could instead solve $\pi(e^{i\theta_0}; z_0, w_0) = 0$ for z_0 and find

$$z_0 = \frac{\rho(e^{i\theta_0}) + w_0\hat{\sigma}(e^{i\theta_0})}{\sigma(e^{i\theta})}.$$

In this case we think of z_0 depending on w_0 and θ_0. For each w consider the curve

$$\Gamma_w : \frac{\rho(\zeta) + w\hat{\sigma}(\zeta)}{\sigma(\zeta)}, \quad \zeta = \exp(i\theta), \quad 0 \le \theta < 2\pi.$$

All boundary points are contained by this curve as well. Since z is real for a fixed w we find θ values such that Γ_w is real, and plot (Γ_w, w).

In figures 3, 4, 5, and 6 the boundary of $\bar{S}$ can be seen by way of both of curves Γ_z and Γ_w. The stability region when $\nu = 0$ is the stability region for CNLF and is shown in figure 3. In this case the A-stability of the IMEX method is guaranteed by the stability of the individual methods CN and LF [FHV96]. This also holds true for energy stability [LT12]. Figure 3 presents a stability region consistent with these results; the stability region is $\{(z, w) : z < 0, \|w\| < 1, \text{w is purely imaginary}\}$.

Figures 4, 5, and 6 show stability regions with smaller time step restrictions than the stability region of CNLF. We find that as ν increases the restriction on the size of w decreases

(hence the restriction on the time step decreases) for all z. When z is small compared to w the value of ν has more of an effect on the size of restriction on w. The boundary curve for $\nu = .1$ in figure 4 does not reach $-i$ or i as in CNLF, but approximately includes the line segment from $-.95i$ to $.95i$. This implies when $z = 0$ a 5% decrease in w is necessary for stability. In figure 5 the stability region contains even less of the imaginary axis. In figure 6 we find a stability region that only contains the portion of the imaginary axis from approximately $-.55i$ to $.55i$ which when $z = 0$ a 45% decrease in w is required for stability.

If we consider the case when z is large (and negative valued) compared to w the value of ν has less of an effect on the size of the restriction on w. In fact as $z \to -\infty$ the stability regions shown in figures 4, 5 and 6 contain points (z, w) where w satisfies $\|w\| < 1$. This is the same time step restriction as in CNLF.

2.5 NUMERICAL TESTS

Consider the initial value problem:

$$u_t + A(u) + \Lambda(u) = 0, \qquad u(0) = [1, 1]^T. \tag{2.23}$$

We shall test LF+RA filter. Take $\nu = 0.19$, $A = 0$, and

$$\Lambda = \begin{bmatrix} 0 & 15 \\ -15 & 0 \end{bmatrix}$$

so $\|\Lambda\| = 15$. The first approximations, u^1, are computed using the implicit backward Euler method. From [LT12] the time step restriction for stability for LF is

$$\Delta t < 1/\|\Lambda\| \approx 0.0667$$

and from Theorem 2 the time step restriction for energy stability for LF+RA is

$$\Delta t < \sqrt{1-\nu}/\|\Lambda\| = .9/\|\Lambda\| = 0.0600.$$

We take $\Delta t = .91/\|\Lambda\| \approx 0.0607$ in Figure 7 and $\Delta t = .89/\|\Lambda\| \approx 0.0593$ in Figure 8.

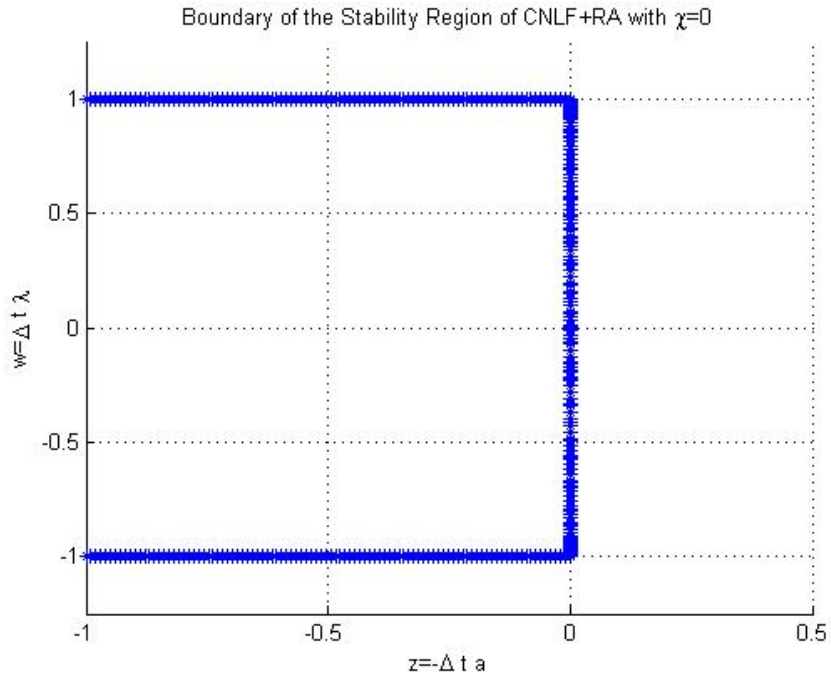

Figure 3: IMEX stability region of CNLF+RA with $\nu = 0$ which is CNLF.

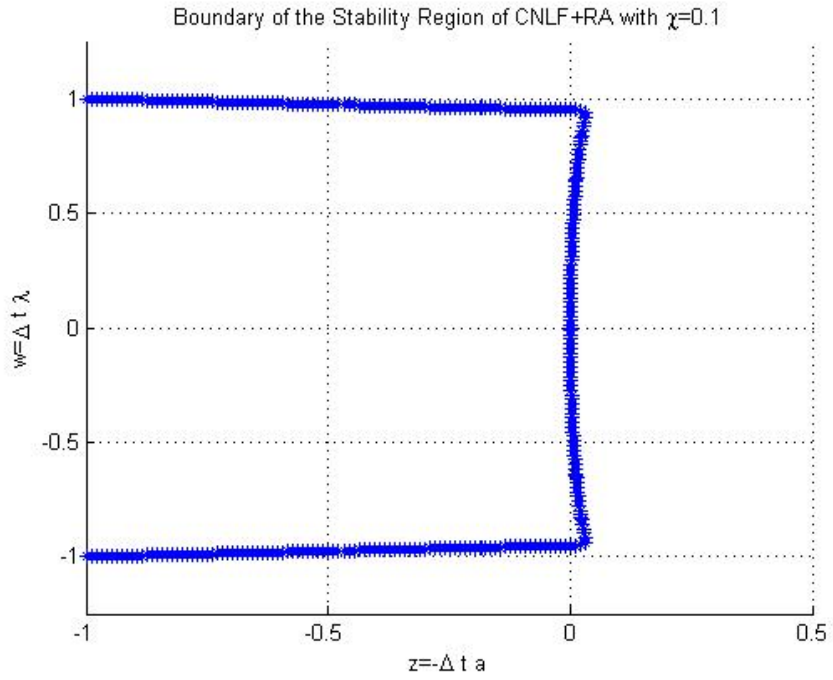

Figure 4: IMEX stability region of CNLF+RA with $\nu = .1$.

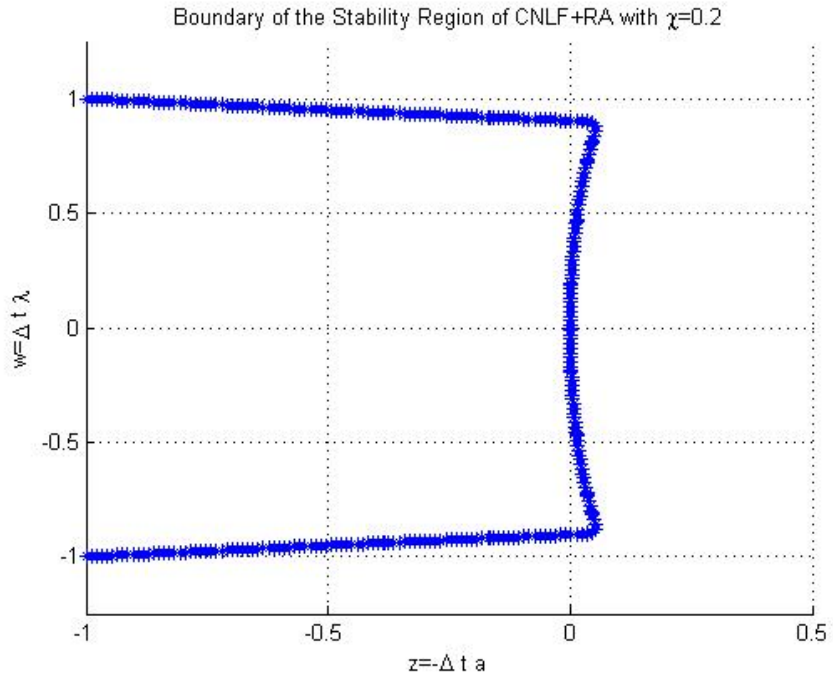

Figure 5: IMEX stability region of CNLF+RA with $\nu = .2$.

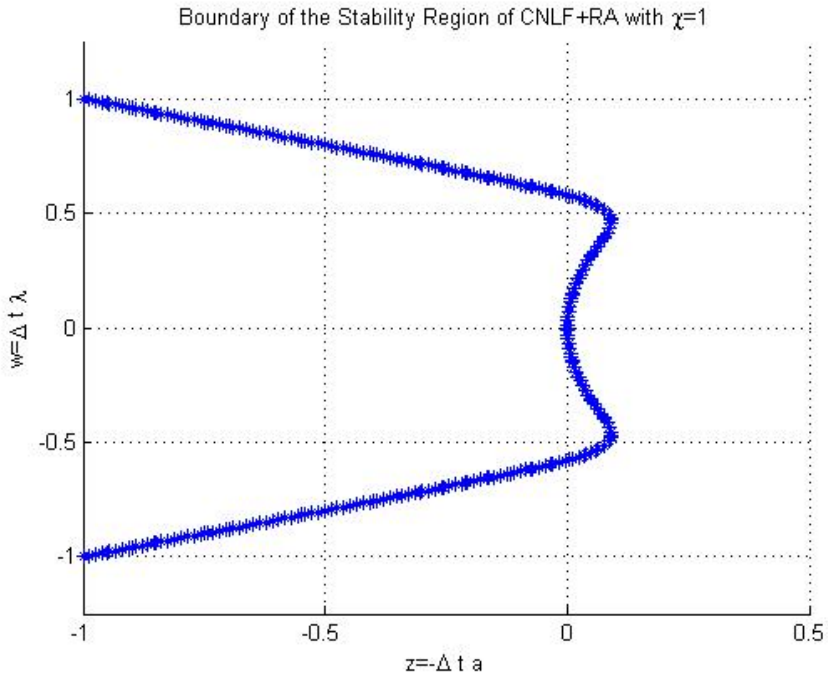

Figure 6: IMEX stability region of CNLF+RA with $\nu = 1$.

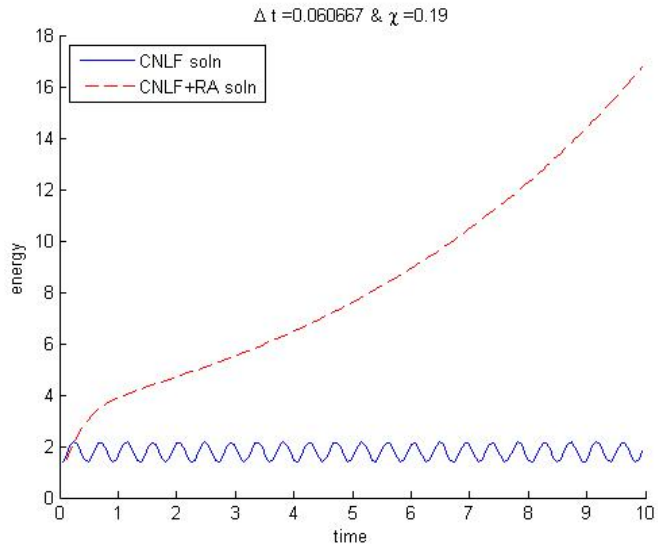

Figure 7: CNLF is stable and CNLF+RA is unstable as anticipated.

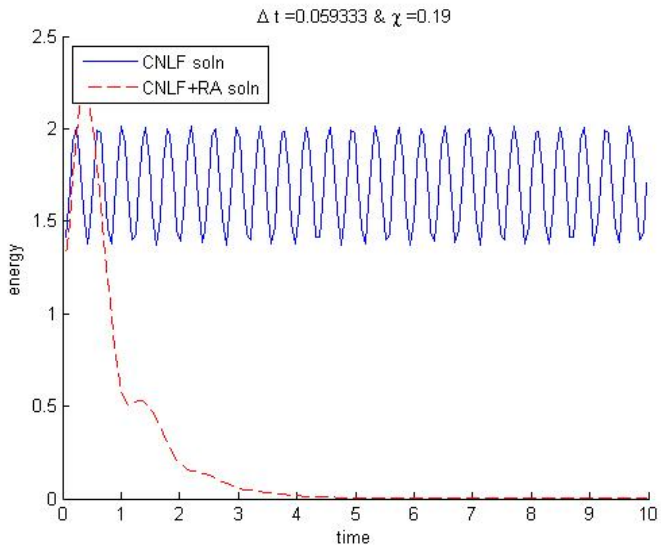

Figure 8: Both CNLF and CNLF+RA are stable with CNLF+RA dissipating to 0.

Since the right hand side of (2.23) is zero any growth is an instability. Here we plot energy $\|u^n\|$ vs. time. We see in both Figures 7 and 8 that the energy of CNLF oscilates but stays bounded as predicted by the stability theory of CNLF. In Figure 7 we confirm energy instability when the time step restriction of Theorem 2 is not satisfied, but in Figure 8 the time step restriction is satified and we observe that the energy is bounded and the energy dissipates.

2.6 CONCLUSIONS

The RA time filter is designed to reduce curvature, and using its curvature reductions properties we find CNLF+RA is equivalent to a linear multistep method. The linear multistep method is stable and dissipates its energy under a time step restriction smaller than CNLF. The stability regions confirm that indeed large ν values require smaller time steps for stability. The numerical tests shows that CNLF+RA is unstable for a small increase in the time

step restriction Δt_{RA} and stable for a slight decrease.

For problems utilizing CNLF in which the spurious mode of LF causes instabilities adding the RA filter will be highly beneficial. The nonphysical energy in the spurios mode is dissipated by the filter and odd and even solutions are prevented from decoupling. But if the stability of the praticular problem we are solving is highly sensitive to the size of the time step restriction then using the RA filter may require too small of a time step for practicality.

Many difficult problems remain open. The W step in the RAW filter antidiffuses the RA filter and therefore can be expected that the analysis of CNLF+RAW will be more delicate than for CNLF+RA. Nevertheless, we are hopeful that, based on the analysis herein, a similar theory could be constructed for the RAW filter, then for more general time filters and finally extended to nonlinear problems.

3.0 STABILITY ANALYSIS OF THE CRANK-NICOLSON-LEAPFROG METHOD WITH THE ROBERT–ASSELIN–WILLIAMS TIME FILTER

3.1 INTRODUCTION

The fundamental method for time stepping in most current geophysical fluid dynamics (GFD) codes consists of one step of the Crank-Nicolson-Leapfrog (CNLF) method (based on a fast-slow wave decoupling strategy) followed by one step of the Robert–Asselin (RA) [R66, A72] time filter to control CNLF's computational mode, and followed by one step of the Williams [W09] time filter to restore lost accuracy and anti-diffuse the RA step. Williams [W09] lists 25 major GFD codes using this approach including the Community Climate Systems Model, e.g., [TL05]. Our goal herein is to complement the numerous numerical tests with a first rigorous numerical analysis of the combination for systems, complementing root condition analysis and numerical tests in, e.g., [D10, W09]. Thus, given $N \times N$ matrices A, Λ, we consider the system for $u : [0, \infty) \to \mathbb{R}^N$

$$\frac{du}{dt} + Au = -\Lambda u, \;\; u(0) = u^0, \text{ where} \tag{3.1}$$

$$A + A^T \geq 0, \text{ and } \Lambda = -\Lambda^T. \tag{3.2}$$

When $A + A^T = 0$ so $A = -A^T$ the system is exactly conservative for the euclidean norm: $|u(t)| = |u(0)|$. When $A + A^T > 0$ it is dissipative, $|u(t)| \to 0$ as $t \to \infty$.

The CNLF method followed by the Robert–Asselin–Williams (RAW) filter [AKW11, W09, W11] is as follows. Given timestep Δt and starting values u^0, v^1 (of sufficient accuracy,

[V09]), find u^n, w^{n+1}, v^{n+1} satisfying

$$\text{(CNLF step)} \qquad \frac{w^{n+1}-u^{n-1}}{2\Delta t} = -A\frac{w^{n+1}+u^{n-1}}{2} - \Lambda v^n, \tag{3.3}$$

$$\text{(RA step)} \qquad u^n = v^n + \frac{\nu\alpha}{2}(w^{n+1} - 2v^n + u^{n-1}), \tag{3.4}$$

$$\text{(W step)} \qquad v^{n+1} = w^{n+1} + \frac{\nu(\alpha-1)}{2}(w^{n+1} - 2v^n + u^{n-1}). \tag{3.5}$$

The parameter ν is the RA filter parameter, usually $\mathcal{O}(0.01 - 0.2)$, and α is the Williams filter parameter, around $1/2$. If $\alpha = 1$ then the W filter step drops out and the method reduces to the CNLF method with the RA filter, and if $\nu = 0$, the unfiltered CNLF scheme is recovered.[1] The unfiltered CNLF method is stable under the time step condition [LT12]

$$\Delta t||\Lambda|| < 1.$$

3.1.1 A summary of results

The computational mode or the unstable mode of CNLF scheme is one for which $u^{n+1} + u^{n-1} \equiv 0$. Difficulties have been reported to appear first in this mode in long-time simulations, e.g., [D10]. There have been many numerical studies of the RAW filter giving evidence of control of CNLF's unstable mode. Our analysis supports this conclusion by showing the stability estimates for the system in Section 3.4 exhibit damping in all modes (see Corollary 1 below).

There have been reports in [DC86], see also [JW11, section 13.5], of stable CNLF simulations that were destabilized when RA step was added. These instabilities (not related to the nonlinear instabilities studied in [F73]) were resolved in [DC86] by cutting the timestep severely. We give two analytic explanations. First, the stability regions of CNLF scheme with the RAW filter in Section 3.5 and the system energy analysis in Theorem 4 lead to

[1] Thus, we assume $\nu \in (0, 1]$ throughout the text.

Courant–Friedrichs–Lewy (CFL) conditions

$$\textbf{(Necessary)}\ \Delta t||\Lambda|| \le CFL_{scalar}(\alpha,\nu),$$
$$\textbf{(Sufficient)}\qquad \Delta t||\Lambda|| \le CFL_{system}(\alpha,\nu),$$
$$\text{where } CFL_{system}(\alpha,\nu) := \sqrt{2\alpha-1}\sqrt{\frac{2-\nu}{\alpha^2(2+\nu-2\alpha\nu)}}\left(1-\frac{\nu}{2}(2\alpha-1)\right),$$
$$CFL_{scalar}(\alpha,\nu) := CFL_{system}(\alpha,\nu)\frac{1}{\sqrt{1-\nu^2(1/2-\alpha)^2}}.$$

The first condition is necessary (and sufficient for scalar problems) while the second is sufficient. The relationship between the conditions is

$$CFL_{system}(\alpha,\nu) \le CFL_{scalar}(\alpha,\nu) < 1 = CFL_{CNLF}.$$

Note that $CFL_{scalar}(\alpha,\nu) \to 0$ as $\alpha \to 1/2$. Thus, a stable CNLF simulation at or near its CFL limit would be exponentially destabilized by an added RAW step.

The natural, but so far unsuccessful, strategy to analyze the stability of the CNLF method with the RAW filter for systems is to track the evolution of a system energy through the individual steps of (3.3), (3.4) and (3.5). Instead, our stability analysis is based on the reduction of the CNLF method with the RAW filter to an equivalent *partitioned multistep method* followed by application of the tools of stability regions and G-stability theory [D78, HW10]. Thus, the first main result is the equivalence to a linear partitioned multistep method and analysis of its consistency error, proved in Section 3.3.

Theorem 3. *The approximation u^n of the CNLF method with the RAW filter satisfies*

$$\begin{aligned} u^n - \nu u^{n-1} - (1-\nu)u^{n-2} =& -\Delta t A(u^n + \nu(\alpha-1)u^{n-1} + (1-\nu\alpha)u^{n-2}) \\ & -\Delta t\Lambda\Big(\big(2+\nu(\alpha-1)\big)u^{n-1} - \nu\alpha u^{n-2}\Big). \end{aligned} \tag{3.6}$$

The the CNLF method with the RAW filter scheme is first-order accurate for $\nu \in (0,1], \alpha \in (1/2,1]$, and is second order when $\alpha = 1/2$.

For notational simplicity, denote γ, p, q, r by

$$\gamma = \nu\sqrt{(1-\alpha)^2 + \alpha^2\Delta t^2\|\Lambda\|^2}, \quad p = 1 - \frac{\gamma}{2}, \tag{3.7}$$
$$q = 1 - \frac{\gamma}{2} - \nu\left(1 - \frac{\nu}{2}\right), \quad r = \sqrt{(\gamma-\nu)^2 + ((2-\nu)\Delta t\|\Lambda\|)^2}.$$

There holds $p > r^2/(4q)$ for $\alpha \in [1/2, 1]$ and $\nu \in (0, 1]$. Our main result, which will be proved in Section 3.4, is as follows.

Theorem 4. *Consider the the CNLF method with the RAW filter (3.3)-(3.5) with $\alpha \in [1/2, 1]$ and $\nu \in (0, 1]$. Suppose that the time step condition holds*

$$\Delta t\|\Lambda\| \le CFL_{system}(\alpha, \nu), \tag{3.8}$$

then the method (3.3)-(3.5) is stable. More precisely, for each $N \ge 2$ we have

$$\begin{aligned}
&\Big(p - \frac{r^2}{4q}\Big)|u^n|^2 + \Big(\frac{r}{2\sqrt{q}}|u^n| - \sqrt{q}|u^{n-1}|\Big)^2 \\
&+ \frac{\gamma}{2}\sum_{n=2}^{N}\big(|u^n - u^{n-1}| - |u^{n-1} - u^{n-2}|\big)^2 + \Big(\frac{\nu}{2}(2\alpha - \nu(2\alpha-1)) - \gamma\Big)\sum_{n=2}^{N-1}|u^n - u^{n-1}|^2 \\
&+ \Delta t\sum_{n=2}^{N}\|u^n + \nu(\alpha-1)u^{n-1} + (1-\nu\alpha)u^{n-2}\|_A^2 \\
&\le |u^1|^2 + |u^0|^2 + (2-\nu)\Delta t\langle\Lambda u^0, u^1\rangle + \frac{\gamma}{2}|u^1 - u^0|^2.
\end{aligned} \tag{3.9}$$

This theorem implies the control of the unstable mode when $A + A^T > 0$.

Corollary 1. *Assume $\Delta t\|\Lambda\| \le CFL_{system}(\alpha, \nu)$ and $A + A^T > 0$. Then the approximations generated by the CNLF method with the RAW filter satisfy $u^n \to 0$ as $n \to \infty$.*

Proof. The right-hand side of (3.9) is independent of N. Thus, letting $N \to \infty$, the infinite series on the left-hand side of (3.9) converge. Hence, the n^{th} terms of all three series must approach zero as $n \to \infty$. Since $A + A^T > 0$, as $n \to \infty$ this implies

$$\begin{aligned}
a_n &= u^n - u^{n-1} \to 0, \\
b_n &= u^n + \nu(\alpha-1)u^{n-1} + (1-\nu\alpha)u^{n-2} \to 0.
\end{aligned}$$

From these two sequences, form the sequence that must also approach zero: $b_n - \nu\alpha a_{n-1} - (a_n - a_{n-1}) = (2-\nu)u^{n-1} \to 0$. □

The stability bound (3.9) and the proof of the corollary shows the mechanism by which RAW controls the unstable mode of CNLF. The second dissipative term controls all modes except those for which $u^n - u^{n-1} \equiv 0$ while the third dissipative term controls all modes except those for which $u^n + \nu(\alpha - 1)u^{n-1} + (1 - \nu\alpha)u^{n-2} \equiv 0$. In combination, both modes are controlled.

The paper is organized as follows. A brief background on the RAW time filter is discussed in Section 3.2. In Section 3.3 and 3.4, we prove Theorem 3 and Theorem 4, respectively. The stability of the leapfrog scheme with RAW filter (i.e., $A = 0$) is given in Section 3.5 using the root locus curve method. The conclusions appear in Section 3.6.

3.2 BACKGROUND ON THE RAW TIME FILTER

Detailed background for the CNLF method with the RAW filter is given in, e.g., [R69, R66, A72, W09, W11, AKW11]. Thus, we give only a brief outline in this section. In GFD simulations the choice of the terms A, Λ in (1.1) is to associate Λu with Coriolis terms yielding waves that are high energy but slow waves, and Au with low energy but fast waves along with other effects. Thus the CFL condition associated with explicit treatment of Λu is modest. Durran [D10, page 412] shows that accuracy degrades rapidly when fully implicit treatment of all terms is used in conjunction with a larger time step violating the timestep condition for the high energy components (see also [L07, K02, HW80]).

The CNLF method has a long history. Stability was proven by Fourier methods in 1963 [JK63] and in 2012 by energy methods for systems, [LT12]. In practical computations with unfiltered CNLF method, non-physical growth in the unstable or computational mode is often reported (e.g., [HV03] and [GS98, page 242]). Computational tests including the RA or RAW time filter report that this growth, whatever its cause, is controlled by the addition of time filters. While the RA filter controls the unstable mode, it also reduces the accuracy from second order (for CNLF) to first order and over damps [LT14, W09, W13]. The computed solution using CNLF method with the RA filter satisfies $u^n \to 0$, even when $||u(t)|| \equiv ||u(0)||$. The W step anti-diffuses the RA step and restores accuracy to the second

order if $\alpha = 1/2 + \mathcal{O}(\Delta t)$.

3.2.1 Curvature evolution

This section reviews the geometric interpretation of the RAW filter in terms of curvature evolution by Robert, Asselin and Williams [W09].

Definition 2. *The discrete curvature of ϕ^n is*

$$\kappa(\phi^n) = \phi^{n+1} - 2\phi^n + \phi^{n-1}.$$

Denote a curvature in time before and after the time filter, (3.4) and (3.5), as, respectively,

$$\begin{aligned} \kappa^n_{old} &= w^{n+1} - 2v^n + u^{n-1}, \\ \kappa^n_{new} &= v^{n+1} - 2u^n + u^{n-1}. \end{aligned}$$

Figure 9 illustrates how the time filter reduces the discrete curvature of the solution. After solving for w^{n+1} in the CNLF step (3.3) the first solution curve is the continuous line. The curvature obtained is κ^n_{old}. Next, performing the filter (3.4) and (3.5) leads to the new solution curve (the dashed line of Figure 9), with curvature κ^n_{new}.

Proposition 3. *For $n \geq 1$ we have*

$$\begin{aligned} \kappa^n_{new} &= (1 - \nu\frac{\alpha+1}{2})\kappa^n_{old}, \\ |\kappa^n_{new}| &< |\kappa^n_{old}| \quad \textit{for } 0 < \nu < 1, 1/2 < \alpha \leq 1. \end{aligned}$$

When $\alpha = 1/2$ the approximated solution computed by the CNLF method with the RAW filter preserves the mean of the solution curves:

$$\frac{v^{n+1} + u^n + u^{n-1}}{3} = \frac{w^{n+1} + v^n + u^{n-1}}{3}.$$

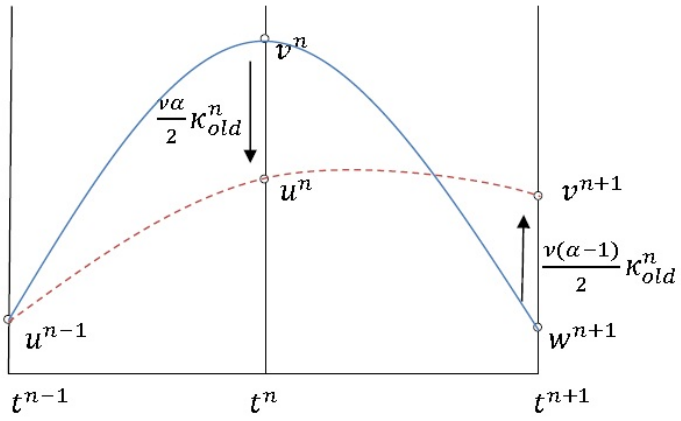

Figure 9: **RA** moves v^n down to decrease κ; **W** moves w^{n+1} to preserve means.

Proof. The first step of the filter (3.4) is $u^n = v^n + \frac{\nu\alpha}{2}\kappa^n_{old}$ and the second step (3.5) is $v^{n+1} = w^{n+1} + \frac{\nu(\alpha-1)}{2}\kappa^n_{old}$. A calculation with (3.4) and (3.5) shows

$$\begin{aligned}
\kappa^n_{new} &= v^{n+1} - 2u^n + u^{n-1} \\
&= (w^{n+1} - 2v^n + u^{n-1}) + (v^{n+1} - w^{n+1}) + 2(v^n - u^n) \\
&= \kappa^n_{old} + \frac{\nu(\alpha-1)}{2}\kappa^n_{old} + 2(\frac{-\nu\alpha}{2})\kappa^n_{old} \\
&= (1 - \frac{\nu(\alpha+1)}{2})\kappa^n_{old}.
\end{aligned}$$

When $\alpha = 1/2$ the means are

$$\frac{v^{n+1} + u^n + u^{n-1}}{3} = \frac{w^{n+1} + v^n + u^{n-1} + \frac{(2\alpha-1)\nu}{2}\kappa^n_{old}}{3} = \frac{w^{n+1} + v^n + u^{n-1}}{3}.$$

□

3.3 THE EQUIVALENT IMEX MULTISTEP METHOD

The identification of the equivalent IMEX multistep method is the first step in the stability analysis. Tools from the theory of such methods will then be applied.

Proof of Theorem 3. This equivalence is proven by algebraic elimination of intermediate variables. Indeed, the first two steps, (3.3) and (3.4), can be rewritten as a block 2x2 system

$$\begin{bmatrix} (I+\Delta t A) & 2\Delta t\Lambda \\ \frac{\nu\alpha}{2} I & (1-\nu\alpha)I \end{bmatrix} \begin{bmatrix} w^{n+1} \\ v^n \end{bmatrix} = \begin{bmatrix} (I-\Delta t A)\, u^{n-1} \\ u^n - \frac{\nu\alpha}{2} u^{n-1} \end{bmatrix}.$$

We solve this system expressing w^{n+1}, v^n in terms of u^n, u^{n-1}. Next these are inserted into (3.5) yielding the claimed linear partitioned multistep method.

Let u be the exact solution of $u'(t) = -Au - \Lambda u$. Using Taylor expansion, the local truncation error of the scheme (3.6) is

$$\begin{aligned} \tau_n(\Delta t) =& \Big| \frac{u(t^n) - \nu u(t^{n-1}) - (1-\nu)u(t^{n-2})}{\Delta t} \\ &+ A\Big(u(t^n) + \nu(\alpha-1)u(t^{n-1}) + (1-\nu\alpha)u(t^{n-2})\Big) \\ &+ \Lambda\Big((2+\nu(\alpha-1))u(t^{n-1}) - \nu\alpha u(t^{n-2})\Big)\Big| \\ =& \frac{\nu}{2}(2\alpha-1)|u'(t^n)|\Delta t + \mathcal{O}(\Delta t^2). \end{aligned}$$

Thus, the method is second order for either $\alpha = 1/2$ or $\nu(\alpha - 1/2) = \mathcal{O}(\Delta t)$, which completes the proof. □

Remark 4 (On parameter values)**.** *The question arises if similar effects can be obtained by using only the RA filter (i.e., $\alpha = 1$ and no W step) but taking smaller parameter values. This does not seem to be the case. Typical values for the RA parameter ν vary from $\nu = 0.01$ in quasi-geostrophic models [W09, S10], to $\nu = 0.12$ for global atmospheric models, to $\nu = 0.5 - 0.6$ for convective cloud models [D10, PX09]. The CNLF method with the RA filter is more stable than with the RAW filter, see e.g., Figure 10. CNLF with either RA or RAW is first order (for $\alpha > 1/2$). However, the consistency error when using the RAW filter has a smaller error coefficient. For example, suppose the RA parameters $\nu = 0.2$, $\alpha = 0.53$. If we then apply only one RA step with $\nu_{RA-new} = \nu(\alpha - 1/2) = 0.006$, then this RA-new*

and RAW have the same order of accuracy and the same coefficient of Δt in the consistency error. However, the value 0.006 *lies outside the range observed in practice of acceptable RA filter values (the associated damping rate is* $1 - \nu_{RA-new} = 0.994 \approx 1$*).*

3.4 G-STABILITY ANALYSIS OF CNLF METHOD WITH THE RAW TIME FILTER

For vectors of the same length, denote the usual euclidean inner product and norm by $\langle u, v\rangle := u^T v$, $|u|^2 := \langle u, u\rangle$, the weighted norm by $\|u\|_A^2 := u^T A u$ (well-defined since $A + A^T > 0$), and by $\|\Lambda\|$ the matrix norm of Λ. In this section, we give the proof of Theorem 4.[2]

Proof. Proof of [Theorem 4] First, we introduce some notation to simplify the proof.

$$\eta^n = u^n - u^{n-1},$$
$$x = \frac{1}{2}\sqrt{\frac{\nu}{2}(2 + \nu - 2\alpha\nu)}, \qquad y = \frac{1}{2}\sqrt{\frac{\nu}{2}(2-\nu)(2\alpha - 1)},$$
$$\gamma = \sqrt{4(x^2 - y^2)^2 + (\alpha\nu\Delta t\|\Lambda\|)^2}, \quad p = 1 - \frac{\gamma}{2},$$
$$q = 1 - \frac{\gamma}{2} - 4x^2 - \nu^2(\alpha - 1), \qquad r = \sqrt{\left(\nu(\alpha - 2) + 2(x^2 - y^2) + \gamma\right)^2 + \left((2-\nu)\Delta t\|\Lambda\|\right)^2},$$

$$\text{and} \quad G = \begin{pmatrix} 1 - (x+y)^2, & \frac{\nu}{2}(\alpha - 2) + 2x(x+y) \\ \frac{\nu}{2}(\alpha - 2) + 2x(x+y), & 1 - (x+y)^2 - 4x^2 - \nu^2(\alpha - 1) \end{pmatrix}.$$

The variables γ, p, q, r are exactly those defined in (3.7). For $\alpha \in [1/2, 1]$ and $\nu \in (0, 1]$, all the variables (except η^n) are non-negative, $x \geq y \geq 0$, and the matrix G is positive definite.

Taking the inner product of (3.6) with $(u^n + \nu(\alpha - 1)u^{n-1} + (1 - \nu\alpha)u^{n-2})$, we have the following identity.

[2]For detailed proof, see the expanded version at http://www.mathematics.pitt.edu/sites/default/files/research-pdfs/CNLFraw.pdf

$$
\begin{aligned}
0 = &\left(\left\| \begin{matrix} u^n \\ u^{n-1} \end{matrix} \right\|_G^2 + (2-\nu)\Delta t \langle \Lambda u^{n-1}, u^n \rangle \right) - \left(\left\| \begin{matrix} u^{n-1} \\ u^{n-2} \end{matrix} \right\|_G^2 + (2-\nu)\Delta t \langle \Lambda u^{n-2}, u^{n-1} \rangle \right) \\
&+ \Delta t \| u^n + \nu(\alpha-1)u^{n-1} + (1-\nu\alpha)u^{n-2} \|_A^2 + |(x+y)u^n - 2xu^{n-1} + (x-y)u^{n-2}|^2 \\
&+ \alpha\nu\Delta t \left(\langle \Lambda u^{n-1}, u^n \rangle - \langle \Lambda u^{n-2}, u^n \rangle + \langle \Lambda u^{n-2}, u^{n-1} \rangle \right). \qquad (3.10)
\end{aligned}
$$

It is easy to check that the last two terms in (3.10) are bounded below by

$$
\begin{aligned}
&|(x+y)u^n - 2xu^{n-1} + (x-y)u^{n-2}|^2 + \alpha\nu\Delta t \Big(\langle \Lambda u^{n-1}, u^n \rangle - \langle \Lambda u^{n-2}, u^n \rangle + \langle \Lambda u^{n-2}, u^{n-1} \rangle \Big) \\
&\geq \left(2(x^2+y^2) - \frac{\gamma}{2} \right) |\eta^n|^2 - \frac{\gamma}{2} |\eta^{n-1}|^2 + \frac{\gamma}{2} \big(|\eta^n| - |\eta^{n-1}| \big)^2 - (x-y)^2 \big(|\eta^n|^2 - |\eta^{n-1}|^2 \big).
\end{aligned}
$$

Inserting this inequality into (3.10), we have

$$
\begin{aligned}
&\left(\left\| \begin{matrix} u^n \\ u^{n-1} \end{matrix} \right\|_G^2 + (2-\nu)\Delta t \langle \Lambda u^{n-1}, u^n \rangle - (x-y)^2 |\eta^n|^2 \right) \\
&\quad + \Delta t \| u^n + \nu(\alpha-1)u^{n-1} + (1-\nu\alpha)u^{n-2} \|_A^2 \\
&\quad + \left(2(x^2+y^2) - \frac{\gamma}{2} \right) |\eta^n|^2 - \frac{\gamma}{2} |\eta^{n-1}|^2 + \frac{\gamma}{2} \left(|\eta^n| - |\eta^{n-1}| \right)^2 \\
&\leq \left(\left\| \begin{matrix} u^{n-1} \\ u^{n-2} \end{matrix} \right\|_G^2 + (2-\nu)\Delta t \langle \Lambda u^{n-2}, u^{n-1} \rangle - (x-y)^2 |\eta^{n-1}|^2 \right). \qquad (3.11)
\end{aligned}
$$

Summing (3.11) for $n = 2$ to N and simplifying it gives

$$
\begin{aligned}
&\left(\left\| \begin{matrix} u^N \\ u^{N-1} \end{matrix} \right\|_G^2 + (2-\nu)\Delta t \langle \Lambda u^{N-1}, u^N \rangle + \left((x+y)^2 - \frac{\gamma}{2} \right) |\eta^N|^2 \right) \\
&\quad + \Delta t \sum_{n=2}^{N} \| u^n + \nu(\alpha-1)u^{n-1} + (1-\nu\alpha)u^{n-2} \|_A^2 + \frac{\gamma}{2} \sum_{n=2}^{N} \left(|\eta^n| - |\eta^{n-1}| \right)^2 \\
&\quad + \left(2(x^2+y^2) - \gamma \right) \sum_{n=2}^{N-1} |\eta^n|^2 \\
&\leq \left\| \begin{matrix} u^1 \\ u^0 \end{matrix} \right\|_G^2 + (2-\nu)\Delta t \langle \Lambda u^0, u^1 \rangle + \frac{\gamma}{2} |\eta_1|^2 \\
&\leq |u^1|^2 + |u^0|^2 + (2-\nu)\Delta t \langle \Lambda u^0, u^1 \rangle + \frac{\gamma}{2} |\eta_1|^2. \qquad (3.12)
\end{aligned}
$$

The first term on the left-hand side of (3.12) is bounded below by

$$\begin{aligned}
&\left\| \begin{array}{c} u^N \\ u^{N-1} \end{array} \right\|_G^2 + (2-\nu)\Delta t\langle \Lambda u^{N-1}, u^N\rangle + \Big((x+y)^2 - \frac{\gamma}{2}\Big)|\eta^N|^2 \\
&\geq \Big(p - \frac{r^2}{4q}\Big)|u^N|^2 + \left(\frac{r}{2\sqrt{q}}|u^N| - \sqrt{q}|u^{N-1}|\right)^2,
\end{aligned}$$

where $4pq > r^2$ for $\alpha \in [1/2, 1]$ and $\nu \in (0, 1]$. Therefore (3.12) becomes

$$\begin{aligned}
&\Big(p - \frac{r^2}{4q}\Big)|u^N|^2 + \left(\frac{r}{2\sqrt{q}}|u^N| - \sqrt{q}|u^{N-1}|\right)^2 \\
&\quad + \Delta t \sum_{n=2}^{N} \|u^n + \nu(\alpha-1)u^{n-1} + (1-\nu\alpha)u^{n-2}\|_A^2 + \frac{\gamma}{2}\sum_{n=2}^{N}\left(|\eta_n| - |\eta^{n-1}|\right)^2 \\
&\quad + \big(2(x^2+y^2) - \gamma\big)\sum_{n=2}^{N-1}|\eta^n|^2 \\
&\leq |u^1|^2 + |u^0|^2 + (2-\nu)\Delta t\langle \Lambda u^0, u^1\rangle + \frac{\gamma}{2}|\eta_1|^2. \qquad (3.13)
\end{aligned}$$

Under the time step condition (3.8), all terms on the left-hand side of (3.13) are positive. Finally, we write (3.13) in terms of α, ν and u^n to obtain the energy bound (3.9). This concludes the proof. □

Remark 4.1 In the case when $\Lambda = 0$ and A is symmetric positive definite, there holds

$$\left\| \begin{array}{c} u^n \\ u^{n-1} \end{array} \right\|_G \leq R(\Delta t A) \left\| \begin{array}{c} u^{n-1} \\ u^{n-2} \end{array} \right\|_G^2,$$

where $0 < R(\Delta t A) < 1$ for any $\Delta t > 0$.

Proof. If $\Lambda = 0$, without loss of generality, let A be a diagonal matrix, i.e., A=diag$(\lambda_1, \cdots, \lambda_N)$, $\lambda_k > 0, k = 1, 2, \cdots, N$. Then we can analyze the system in terms of components. One can derive that the k^{th} component of the numerical solution satisfies $u_{(k)}^n = R(\Delta t\lambda_k)u_{(k)}^{n-1}$, where

$$\begin{aligned}
&R(\Delta t\lambda_k) = \\
&\frac{(\nu + \nu(1-\alpha)\Delta t\lambda_k) \pm \sqrt{(\nu + \nu(1-\alpha)\Delta t\lambda_k)^2 + 4(1+\Delta t\lambda_k)(1-\nu-(1-\nu\alpha)\Delta t\lambda_k)}}{2(1+\Delta t\lambda_k)}.
\end{aligned}$$

This yields

$$\left\| \begin{array}{c} u^n_{(k)} \\ u^{n-1}_{(k)} \end{array} \right\|_G = |R(\Delta t \lambda_k)| \left\| \begin{array}{c} u^{n-1}_{(k)} \\ u^{n-2}_{(k)} \end{array} \right\|_G^2 .$$

It is easy to check that $|R(\Delta t \lambda_k)| < 1$ for $k = 1, \cdots, N$. By letting

$$R(\Delta t A) = \max_{1 \le k \le N} |R(\Delta t \lambda_k)|,$$

we conclude the proof.

□

Corollary 2. *When $\alpha = 1$ the resulting CNLF method with the RA filter with $\nu \in (0, 1]$ is stable if*

$$\Delta t \|\Lambda\| \le 1 - \nu/2.$$

3.5 ABSOLUTE STABILITY REGION AND ROOT LOCUS CURVE OF LEAPFROG SCHEME WITH RAW TIME FILTER

Stability can be analyzed exactly for scalar problems following the root locus curve method. The results of this analysis are organized in a compact and useful manner by the stability regions, derived in this section.

3.5.1 Root locus curve

Taking $A = 0$, we consider the leapfrog method with the RAW filter. In this case (3.6) becomes

$$u^n - \nu u^{n-1} - (1 - \nu) u^{n-2} = -\Delta t \Lambda \Big(\big(2 + \nu(\alpha - 1)\big) u^{n-1} - \nu \alpha u^{n-2} \Big). \tag{3.14}$$

The characteristic polynomials of (3.14) are

$$\rho(\zeta) = \zeta^2 - \nu\zeta - (1 - \nu),$$
$$\sigma(\zeta) = -(2 + \nu(\alpha - 1))\zeta + \nu\alpha.$$

Denote $w = \Delta t\lambda$, where λ is an arbitrary non-zero eigenvalue of Λ. Thus, w is a purely imaginary number. Let ζ be on the unit circle, i.e., $\zeta = e^{i\theta}$, $\theta \in [0, 2\pi]$, then the characteristic equation of (3.14) is

$$\rho(\zeta) - w\sigma(\zeta) = 0 \quad \text{or} \quad w = \frac{\rho(\zeta)}{\sigma(\zeta)}.$$

Since w is purely imaginary, the real part of w is zero. Consequently, θ satisfies

$$\cos\theta = 1 \text{ or } \cos\theta = \nu - 1 + \frac{2-\nu}{2\alpha},$$

and hence

$$w = 0, \text{ or, } w = \pm i\frac{\sqrt{(2-\nu)(2\alpha-1)}}{\alpha\sqrt{2-\nu+2\alpha\nu}}.$$

The values above indicate the intersections of the root locus curve with the imaginary axis. Since λ is an arbitrary non-zero eigenvalue of Λ, the stability region is given by

$$\Delta t\|\Lambda\| \leq \frac{\sqrt{(2-\nu)(2\alpha-1)}}{\alpha\sqrt{2-\nu+2\alpha\nu}} = CFL_{scalar}(\alpha, \nu).$$

Therefore we have proven the following result on the absolute stability of the leapfrog method with the RAW time filter.

Proposition 4. *The leapfrog method with the RAW filter (i.e., $A = 0$) is stable if and only if the time step condition satisfies*

$$\Delta t||\Lambda|| \leq CFL_{scalar}(\alpha, \nu). \tag{3.15}$$

Several root locus curves for the leapfrog method with the RAW filter are plotted in Figure 10. For a fixed value ν, the intersection of the root locus curve with the imaginary axis shrinks as α decreases.

Corollary 3. *The leapfrog method with the RAW filter for $\alpha = 1/2$ is unstable for $\nu \in (0, 1]$.*

Proof. From (3.15) we note that $CFL_{scalar}(\alpha, \nu) = 0$ when $\alpha = 1/2$. This implies that the only intersection of the root locus curve with the imaginary axis is the origin, concluding the argument.

□

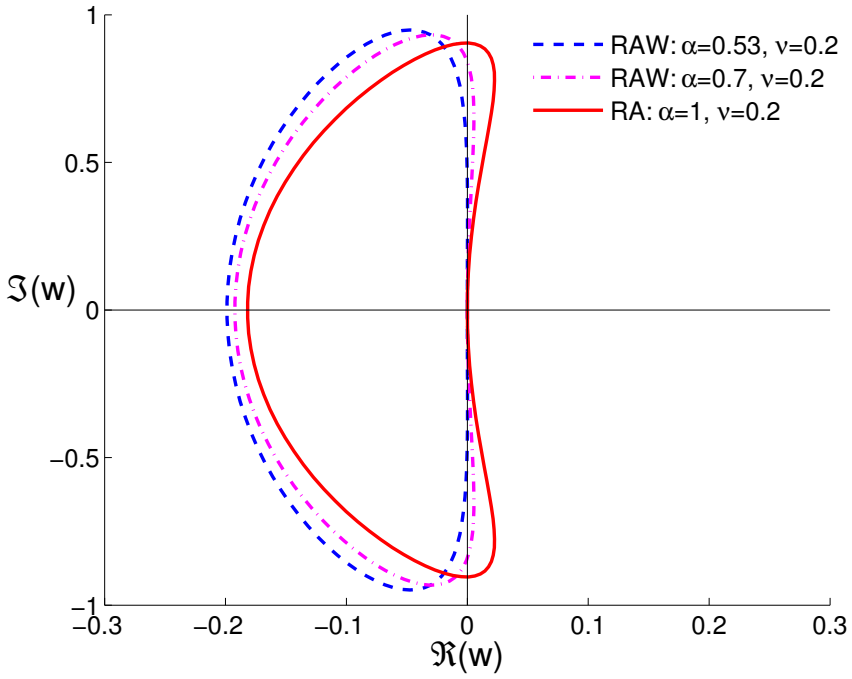

Figure 10: Root locus curves of the leapfrog method with the RAW filter for $\alpha = 0.53, 0.7, 1$, with a fixed value $\nu = 0.2$.

Corollary 4. *Let $A = 0, \Lambda \neq 0$. Then, the CNLF method with the RAW filter is unconditionally unstable if $\alpha = 1/2$.*

Proof. Two different proofs: First, the stability region of the CNLF method with the RAW filter does not intersect the imaginary axis if $\alpha = 1/2$. Second, in the above necessary condition for stability $CFL_{scalar}(\alpha, \nu) = 0$ if $\alpha = 1/2$. □

This corollary is one explanation of the common practice[3] of taking $\alpha > 1/2$ but close to $\alpha = 1/2$.

We give an illustration showing the energy behavior for different time steps. Consider

$$u'(t) = \Lambda u(t), \quad \Lambda = \begin{pmatrix} 0 & 10 \\ -10 & 0 \end{pmatrix}, \quad u(0) = [1, 1]^T.$$

Take $\alpha = 0.53$ and $\nu = 0.2$, and denote the time step threshold in (3.15) as Δt_{RAW}, i.e., $\Delta t_{RAW} = CFL_{scalar}/\|\Lambda\|$. The energy of the numerical solution for $\Delta t = 1.01\Delta t_{RAW}$, $\Delta t = \Delta t_{RAW}$ and $\Delta t = 0.99\Delta t_{RAW}$ is plotted in Figure 11. The time step condition (3.15) is sharp, and a smaller (bigger) time step with respect to the threshold will force the numerical solution stable (unstable).

3.6 CONCLUSIONS

The Crank-Nicolson-Leapfrog method with the Robert-Asselin-Williams time filter is equivalent to an implicit-explicit combination of a linear multistep method. We derived the method's stability regions for scalar cases and performed the G-stability analysis for systems. The RAW filter stabilizes the unstable or computational mode of the CNLF method.

[3]Thus, the recommendation $\alpha = 1/2$ is shorthand for, e.g., $\alpha = 1/2 + \mathcal{O}(\Delta t)$, which also preserves the higher consistency error of $\alpha = 1/2$.

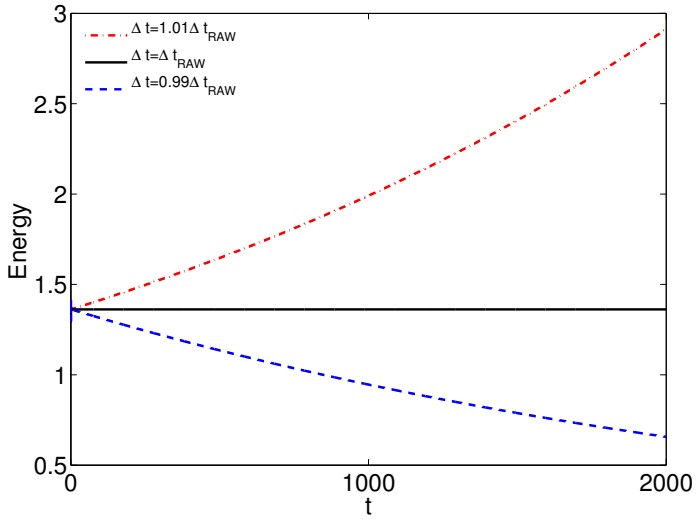

Figure 11: Energy of the numerical solution for different time steps. The energy grows for $\Delta t = 1.01\Delta t_{RAW}$, decays for $\Delta t = 0.99\Delta t_{RAW}$ and stays preserved for $\Delta t = \Delta t_{RAW}$.

4.0 THE UNSTABLE MODE IN THE CRANK-NICOLSON LEAP-FROG METHOD IS STABLE

4.1 INTRODUCTION

In this chapter we prove (asymptotic) stability of the so-called *unstable mode* (or *computational mode*) of the Crank-Nicolson Leap-Frog, CNLF, method for:

$$\begin{aligned} &\frac{du}{dt} + Au + \Lambda u = 0, \text{ for } t > 0 \text{ and } u(0) = u_0 \\ &A : A + A^T > 0 \text{ and } \Lambda : \text{ skew symmetric.} \end{aligned} \tag{4.1}$$

Here $u : [0, \infty) \to \mathbb{R}^d$ and the square, non-commutative, real matrices A, Λ have compatible dimensions. Under these conditions, the solution to (4.1) satisfies $u(t) \to 0$ as $t \to \infty$ so any growth in the approximate solution is a numerics induced instability. With superscript denoting the time step number, CNLF, the Implicit-Explicit (IMEX) combination of Crank-Nicolson and Leap Frog, is given by: given u^0, u^1, for $n \geq 2$

$$\frac{u^{n+1} - u^{n-1}}{2\triangle t} + A\frac{u^{n+1} + u^{n-1}}{2} + \Lambda u^n = 0. \tag{CNLF}$$

Root condition analysis for the scalar test problem $y' + ay + i\lambda y = 0$ leads to the timestep condition, necessary for stability, [JK63], and recently proven sufficient in [LT12],

$$\triangle t|\Lambda| < 1, \quad |\cdot| = \text{euclidean norm.} \tag{4.2}$$

However, in practical simulations, difficulties with CNLF's unstable mode occur. It is often reported that as $n \to \infty$

$$\begin{aligned} &\text{Stable Mode: } |u^{n+1} + u^{n-1}| \to 0, \\ &\text{Unstable Mode: } |u^{n+1} - u^{n-1}| \to \infty. \end{aligned} \tag{4.3}$$

CNLF is used for many geophysical flow simulations from which experience with and fixes for the unstable mode are correspondingly large, e.g., [D10], [K03], [K12], [TL05], [A72], [R69], [W11], [JW11]. One mystery is that since CNLF is stable under (4.2), no growth is possible in theory and yet time filters to deal with (4.3) are nearly universal in practice, [JW11]. It is an open question to determine if this could be due to a gap for IMEX methods (e.g., [ARW95], [CM10], [FHV96], [HV03], [V80], [V09]) between necessary conditions from root condition analysis and sufficient ones for systems, to accumulation in the unstable mode of roundoff errors, to imperfect imposition of the timestep condition, to nonlinearities or other unknown causes. We prove that under (4.2) *the CNLF unstable mode is (asymptotically) stable*. This result, consistent with numerical tests in Section 3, supports the scenario that growth in the unstable mode is due to imperfect imposition of and thus slight violation of (4.2).

Theorem 5. *Suppose the timestep condition (4.2) holds. Then, all modes of CNLF are asymptotically stable:*

$$\begin{aligned} &u^n \to 0 \text{ as } n \to \infty \text{ and thus both} \\ &u^{n+1} + u^{n-1} \to 0 \text{ and } u^{n+1} - u^{n-1} \to 0. \end{aligned}$$

4.2 PROOF OF ASYMPTOTIC STABILITY OF THE UNSTABLE MODE

Denote the usual euclidean inner product and norm by $\langle w, v \rangle := w^T v$, $|v|^2 := \langle v, v \rangle$ and the $A-$norm (well defined since $A + A^T > 0$) by

$$|u|_A^2 := u^T A u.$$

Step 1: Energy Stability. In step 1 we follow [LT12]. Take the inner product of CNLF with $u^{n+1}+u^{n-1}$, add and subtract $|u^{\boldsymbol{n}}|^2$ and multiply through by $2\triangle t$. This yields

$$\begin{aligned}&\left[|u^{n+1}|^2+|u^{\boldsymbol{n}}|^2\right]-\left[|u^{\boldsymbol{n}}|^2+|u^{n-1}|^2\right]\\&+\triangle t|u^{n+1}+u^{n-1}|_A^2+2\triangle t\langle\Lambda u^n,u^{n+1}+u^{n-1}\rangle=0.\end{aligned}\tag{4.4}$$

Next, using skew symmetry rearrange

$$2\triangle t\langle\Lambda u^n,u^{n+1}+u^{n-1}\rangle=2\triangle t\langle\Lambda u^n,u^{n+1}\rangle-2\triangle t\left\langle\Lambda u^{n-1},u^n\right\rangle.$$

Define the first energy (which is positive if $\triangle t|\Lambda|<1$, [LT12])

$$E^{n+1/2}:=|u^{n+1}|^2+|u^n|^2+2\triangle t\langle\Lambda u^n,u^{n+1}\rangle.$$

Collecting terms we obtain

$$E^{n+1/2}-E^{n+1/2}+\triangle t|u^{n+1}+u^{n-1}|_A^2=0.\tag{4.5}$$

This implies that the stable mode $u^{n+1}+u^{n-1}\to 0$ as $n\to\infty$. Indeed, summing for $n=1,\cdots,N$ and then letting $N\to\infty$, we see that

$$\sum\nolimits_{n=1}^{\infty}|u^{n+1}+u^{n-1}|_A^2<\infty$$

and thus the n^{th} term $|u^{n+1}+u^{n-1}|_A^2\to 0$.

Step 2: A second estimate. Take the inner product of CNLF with $u^{n+1}-u^{n-1}$ and multiply through by $2\triangle t\delta$ where $\delta>0$ will be determined later. This gives

$$\begin{aligned}&\triangle t\delta\left\langle A(u^{n+1}+u^{n-1}),u^{n+1}-u^{n-1}\right\rangle\\&+\delta|u^{n+1}-u^{n-1}|^2+2\delta\triangle t\langle\Lambda u^n,u^{n+1}-u^{n-1}\rangle=0.\end{aligned}\tag{4.6}$$

Split the operator A into two parts, $A := A_s + A_{ss}$ where A_s is symmetric and A_{ss} is skew-symmetric. The first term of (4.6) becomes

$$\begin{aligned}
&\left\langle A(u^{n+1}+u^{n-1}), u^{n+1}-u^{n-1}\right\rangle \\
&= \left\langle A_s(u^{n+1}+u^{n-1}), u^{n+1}-u^{n-1}\right\rangle + \left\langle A_{ss}(u^{n+1}+u^{n-1}), u^{n+1}-u^{n-1}\right\rangle \\
&= \left\langle A_s u^{n+1}, u^{n+1}\right\rangle - \left\langle A_s u^{n-1}, u^{n-1}\right\rangle + \left\langle A_{ss}(u^{n+1}+u^{n-1}), u^{n+1}-u^{n-1}\right\rangle \\
&= |u^{n+1}|_A^2 - |u^{n-1}|_A^2 + \left\langle A_{ss}(u^{n+1}+u^{n-1}), u^{n+1}-u^{n-1}\right\rangle
\end{aligned}$$

since the $A-$norm holds the property $|v|_A^2 = \langle A_s v, v\rangle$. Use the above equality for the first term in (4.6) and add and subtract $\triangle t\delta|u^{\boldsymbol{n}}|_A^2$ to gain

$$\begin{aligned}
&\left[\delta\triangle t|u^{n+1}|_A^2 + \delta\triangle t|u^n|_A^2\right] - \left[\delta\triangle t|u^n|_A^2 + \delta\triangle t|u^{n-1}|_A^2\right] \\
&+\delta\triangle t\left\langle A_{ss}(u^{n+1}+u^{n-1}), u^{n+1}-u^{n-1}\right\rangle \\
&+\delta|u^{n+1}-u^{n-1}|^2 + 2\delta\triangle t\langle \Lambda u^n, u^{n+1}-u^{n-1}\rangle = 0.
\end{aligned} \tag{4.7}$$

Define the second energy

$$\mathcal{E}^{n+1/2} := E^{n+1/2} + \delta\triangle t|u^{n+1}|_A^2 + \delta\triangle t|u^n|_A^2.$$

The *key step* is adding (4.5) and (4.7) which gives

$$\begin{aligned}
&\mathcal{E}^{n+1/2} - \mathcal{E}^{n-1/2} + \triangle t|u^{n+1}+u^{n-1}|_A^2 + \delta|u^{n+1}-u^{n-1}|^2 \\
&+\delta\triangle t\left\langle A_{ss}(u^{n+1}+u^{n-1}), u^{n+1}-u^{n-1}\right\rangle + 2\delta\triangle t\langle \Lambda u^n, u^{n+1}-u^{n-1}\rangle = 0.
\end{aligned}$$

Summing this from $n=1$ to N gives

$$\mathcal{E}^{N+1/2} + \sum_{n=1}^{N}\left[\triangle t|u^{n+1}+u^{n-1}|_A^2 + \delta|u^{n+1}-u^{n-1}|^2\right] + Q_1 + Q_2 = \mathcal{E}^{1/2}, \tag{4.8}$$

$$Q_1 := \sum_{n=1}^{N}\delta\triangle t\left\langle A_{ss}(u^{n+1}+u^{n-1}), u^{n+1}-u^{n-1}\right\rangle,$$

$$Q_2 := \sum_{n=1}^{N} 2\delta\triangle t\langle \Lambda u^n, u^{n+1}-u^{n-1}\rangle.$$

Step 3: Bounding $|Q_1|$ & $|Q_2|$. For Q_1 note that

$$\begin{aligned}
&\left\langle A_{ss}(u^{n+1}+u^{n-1}), u^{n+1}-u^{n-1}\right\rangle \\
&\leq |A_{ss}||u^{n+1}+u^{n-1}||u^{n+1}-u^{n-1}| \\
&\leq \frac{1}{2\epsilon}|A_{ss}||u^{n+1}+u^{n-1}|^2+\frac{\epsilon}{2}|A_{ss}||u^{n+1}-u^{n-1}|^2
\end{aligned}$$

where $\epsilon > 0$. Hence

$$|Q_1| \leq \sum_{n=1}^{N}\frac{\delta\triangle t}{2\epsilon}|A_{ss}||u^{n+1}+u^{n-1}|^2+\sum_{n=1}^{N}\frac{\delta\triangle t\epsilon}{2}|A_{ss}||u^{n+1}-u^{n-1}|^2$$

For Q_2 note that

$$\begin{aligned}
&\langle \Lambda u^n, u^{n+1}-u^{n-1}\rangle \\
&\quad= \frac{1}{2}\langle \Lambda(u^n-u^{n-2}), u^{n+1}-u^{n-1}\rangle+\frac{1}{2}\langle \Lambda(u^n+u^{n-2}), u^{n+1}-u^{n-1}\rangle \\
&\quad\leq \frac{1}{2}|\Lambda||u^n-u^{n-2}||u^{n+1}-u^{n-1}|+\frac{1}{2}|\Lambda||u^n+u^{n-2}||u^{n+1}-u^{n-1}| \\
&\quad\leq \frac{1}{2}|\Lambda|\left(\frac{1}{2}|u^n-u^{n-2}|^2+\frac{1}{2}|u^{n+1}-u^{n-1}|^2\right)+ \\
&\qquad\qquad +\frac{1}{2}|\Lambda|\left(\frac{1}{2\epsilon}|u^n+u^{n-2}|^2+\frac{\epsilon}{2}|u^{n+1}-u^{n-1}|^2\right).
\end{aligned}$$

Then

$$\begin{aligned}
2\delta\Delta t\sum_{n=1}^{N}\frac{1}{2}|\Lambda|\left(\frac{1}{2}|u^n-u^{n-2}|^2+\frac{1}{2}|u^{n+1}-u^{n-1}|^2\right) &= \frac{\delta}{2}\Delta t|\Lambda||u^{N+1}-u^{N-1}|^2+ \\
+\delta\Delta t|\Lambda|\left(|u^N-u^{N-2}|^2+\cdots+|u^3-u^1|^2\right)+\frac{\delta}{2}\Delta t|\Lambda||u^2-u^0|^2& \\
\leq \delta\Delta t|\Lambda|\sum_{n=1}^{N}|u^{n+1}-u^{n-1}|^2,& \qquad (4.9)
\end{aligned}$$

and

$$\begin{aligned}
&2\delta\Delta t\sum_{n=1}^{N}\frac{1}{2}|\Lambda|\left(\frac{1}{2\epsilon}|u^n+u^{n-2}|^2+\frac{\epsilon}{2}|u^{n+1}-u^{n-1}|^2\right) \\
=&\frac{\delta\Delta t|\Lambda|}{2\epsilon}\sum_{n=1}^{N-1}|u^{n+1}+u^{n-1}|^2+\frac{\epsilon\delta\Delta t|\Lambda|}{2}\sum_{n=1}^{N}|u^{n+1}-u^{n-1}|^2 \\
\leq&\frac{\delta\Delta t|\Lambda|}{2\epsilon}\sum_{n=1}^{N}|u^{n+1}+u^{n-1}|^2+\frac{\epsilon\delta\Delta t|\Lambda|}{2}\sum_{n=1}^{N}|u^{n+1}-u^{n-1}|^2. \qquad (4.10)
\end{aligned}$$

Thus, $|Q_2|$ is now bounded by combining (4.9) and (4.10) as follows

$$|Q_2| \leq \delta\Delta t|\Lambda|(1+\frac{\epsilon}{2})\sum_{n=1}^{N}|u^{n+1}-u^{n-1}|^2+\frac{\delta\Delta t|\Lambda|}{2\epsilon}\sum_{n=1}^{N}|u^{n+1}+u^{n-1}|^2.$$

Hence

$$|Q_1|+|Q_2| \leq \delta\Delta t\Big(|\Lambda|(1+\frac{\epsilon}{2})+\frac{\epsilon}{2}|A_{ss}|\Big)\sum_{n=1}^{N}|u^{n+1}-u^{n-1}|^2$$
$$+\frac{\delta\Delta t}{2\epsilon}\Big(|\Lambda|+|A_{ss}|\Big)\sum_{n=1}^{N}|u^{n+1}+u^{n-1}|^2.$$

Step 4: Using the Q_1 & Q_2 estimates in the energy inequality. Inserting this estimate for Q_1 and Q_2 into the energy inequality and collecting terms gives

$$\mathcal{E}^{N+1/2}+\delta\left(1-(1+\frac{\epsilon}{2})\Delta t|\Lambda|-\frac{\epsilon}{2}\triangle t|A_{ss}|\Big)\sum_{n=1}^{N}|u^{n+1}-u^{n-1}|^2\right.$$
$$+\Delta t\sum_{n=1}^{N}\left(|u^{n+1}+u^{n-1}|_A^2-\frac{\delta}{2\epsilon}\Big(|\Lambda|+|A_{ss}|\Big)|u^{n+1}+u^{n-1}|^2\right)\leq C(u^0,u^1). \tag{4.11}$$

Step 5: Estimating the unstable mode. Since the RHS, $C(u^0,u^1)$, is independent of N, we can let $N\to\infty$ and conclude that

$$\delta\left(1-(1+\frac{\epsilon}{2})\Delta t|\Lambda|-\frac{\epsilon}{2}\triangle t|A_{ss}|\Big)\sum_{n=1}^{\infty}|u^{n+1}-u^{n-1}|^2+\right.$$
$$+\Delta t\sum_{n=1}^{\infty}\left(|u^{n+1}+u^{n-1}|_A^2-\frac{\delta}{2\epsilon}\left(|\Lambda|+|A_{ss}|\right)|u^{n+1}+u^{n-1}|^2\right)<\infty.$$

From this we shall deduce that $\sum_{n=1}^{\infty}|u^{n+1}-u^{n-1}|^2<\infty$ and thus $|u^{n+1}-u^{n-1}|^2\to 0$ as $n\to\infty$. To make this step, two conditions are required: the second sum must be non-negative and the coefficient of the first sum positive. That coefficient is positive if

$$\epsilon<2\frac{1-\triangle t|\Lambda|}{\triangle t|\Lambda|+\triangle t|A_{ss}|}$$

Since $\epsilon>0$ is arbitrary, this condition can be satisfied if the stability condition $\Delta t|\Lambda|<1$ holds. For the second sum to be non-negative, it suffices that

$$|u^{n+1}+u^{n-1}|_A^2-\frac{\delta\left(|\Lambda|+|A_{ss}|\right)}{2\epsilon}|u^{n+1}+u^{n-1}|^2\geq 0.$$

This can be attained by picking $\delta = \epsilon\lambda_{\min}(A_s)/\left(|\Lambda| + |A_{ss}|\right)$, where $\lambda_{\min}(A_s)$ denotes the minimum eigenvalue of A_s. With this condition on $\triangle t$ and choice of δ, we conclude that the sum below converges

$$\sum_{n=1}^{\infty} |u^{n+1} - u^{n-1}|^2 \leq C < \infty. \tag{4.12}$$

Thus the n^{th} term $|u^{n+1} - u^{n-1}|^2 \to 0$ and $|u^{n+1} + u^{n-1}|_A^2 \to 0$ from Step 1. Hence, $u^n \to 0$ and all modes, including the unstable mode, are controlled.

4.3 NUMERICAL EXPLORATION OF THE UNSTABLE MODE

There are (at least) three natural conjectures about the growth of the unstable mode[1]. The **first** is that practical simulations often occur with many accompanying perturbations. Thus the matrix Λ will only be skew symmetric to $O(\varepsilon)$, where ε is the magnitude of the errors in numerical integration, computer arithmetic, function evaluation, previous calculations and so on used to generate Λ and form the product Λu. These perturb the eigenvalues of Λ to be outside the stability interval of leap-frog, $\{z : \mathrm{Re}(z) = 0, -1 < \mathrm{Im}(z) < +1\}$. CN contributes damping of the stable mode sufficient to control its growth, leaving the unstable mode's growth to accumulate. The **second** is that practical simulations often occur for implicitly defined operators Λ. The singular values of Λ are not available and guesses of $|\Lambda|$ based on physical reasoning or preliminary calculations are used instead. As a result, the timestep condition $\triangle t|\Lambda| < 1$ may be slightly violated. This results in an instability that begins small, is damped in the stable mode by CN and accumulates in the unstable mode. The **third** is that the unstable mode occurs only in cases not covered by the theorem such as with $A = A(u)$. Practical simulations often occur with Λ a linear operator (as covered) but $A = A(u)$ a nonlinear operator with $\langle A(u), u\rangle \geq 0$ for which step 2 in the proof fails.

We give three tests to check these scenarios.

[1]These scenarios owe much to many lively discussions with Catalin Trenchea, for which we are appreciative.

Test 1:A has large skew symmetric part. Let

$$A = \begin{bmatrix} 10^4 & 10^3 \\ -10^3 & 10^{-4} \end{bmatrix}$$

which has symmetric part $A_s = diag\{10^4, 10^{-4}\}$ and skew symmetric part $A_{ss} = antidiag\{-10^3, 10^3\}$ and consider the 2×2 system

$$\frac{du}{dt} + (10^4 u + 10^3 v) - v = 0, \ \frac{dv}{dt} + (10^{-4} v - 10^3 u) + u = 0.$$

The matrix Λ is

$$\Lambda = \begin{bmatrix} 0 & -1 \\ +1 & 0 \end{bmatrix}.$$

We apply CNLF over a long time interval:

$$\begin{aligned} \frac{u^{n+1} - u^{n-1}}{2\triangle t} + 10^4 \frac{u^{n+1} + u^{n-1}}{2} + 10^3 \frac{v^{n+1} + v^{n-1}}{2} - v^n &= 0, \\ \frac{v^{n+1} - v^{n-1}}{2\triangle t} + 10^{-4} \frac{v^{n+1} + v^{n-1}}{2} - 10^3 \frac{u^{n+1} + u^{n-1}}{2} + u^n &= 0, \end{aligned}$$

with starting conditions $u^0 = v^0 = u^1 = +1, v^1 = -1$. We calculate $|\Lambda| = 1$ so the time step condition is $\triangle t < 1$. We test:

- For $\triangle t = 1.01 (> 1)$ CNLF is unstable. Figure 12 verifies that the instability occurs in only the unstable mode (a scenario suggested by root condition analysis [D10]).
- For $\triangle t = 0.99 (< 1)$, CNLF is energy stable. All modes are observed to be stable in figure 15 over a very long time interval.

Test 2: Small perturbations of Λ. Let $A = diag\{10^4, 10^{-4}\}$ and consider the 2×2 system

$$\frac{du}{dt} + 10^4 u + \varepsilon_1 u - v = 0, \ \frac{dv}{dt} + 10^{-4} v + \varepsilon_2 v + u = 0.$$

The matrix Λ is thus

$$\Lambda_{\varepsilon_1, \varepsilon_2} = \begin{bmatrix} \varepsilon_1 & -1 \\ +1 & \varepsilon_2 \end{bmatrix}$$

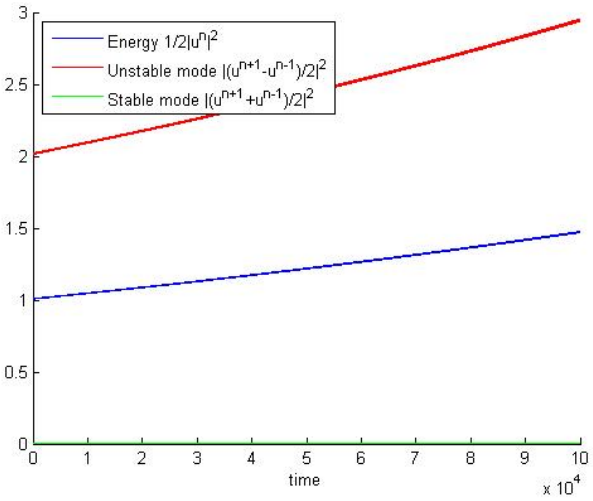

Figure 12: For $\triangle t = 1.01$ the unstable mode grows and the stable mode decays

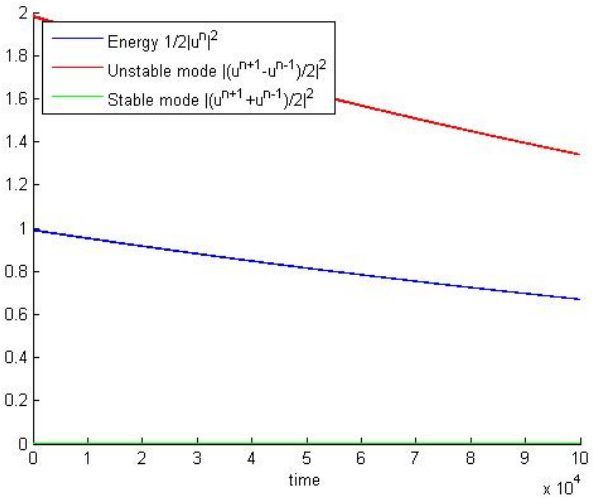

Figure 13: For $\triangle t = .99$ the both unstable and stable modes decay

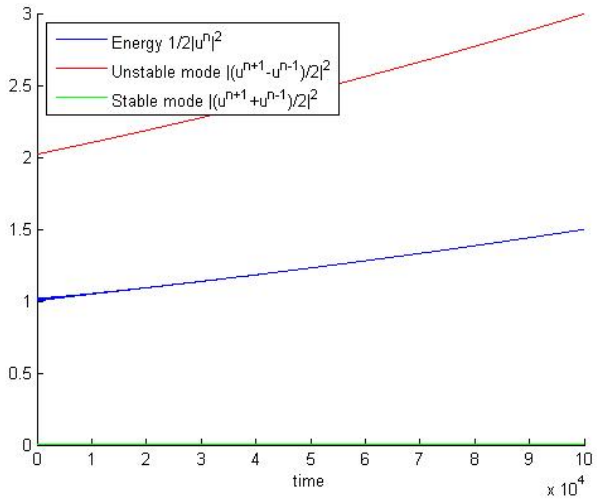

Figure 14: For $\triangle t = 1.01$ the unstable mode grows and the stable mode decays

in which skew symmetry is broken by the small, random coefficients ε_1 and ε_2. We apply CNLF over a long time interval:

$$\begin{aligned} \frac{u^{n+1}-u^{n-1}}{2\triangle t} + 10^4 \frac{u^{n+1}+u^{n-1}}{2} + \varepsilon_1 u^n - v^n &= 0, \\ \frac{v^{n+1}-v^{n-1}}{2\triangle t} + 10^{-4} \frac{v^{n+1}+v^{n-1}}{2} + \varepsilon_2 v^n + u^n &= 0, \end{aligned}$$

with starting conditions $u^0 = v^0 = u^1 = +1, v^1 = -1$. We calculate $|\Lambda_{0,0}| = 1$ so the time step condition is $\triangle t < 1$. We test:

- For $\triangle t = 1.01 (> 1)$ and $\varepsilon_1 = \varepsilon_2 = 0$ CNLF is unstable. Figure 14 verifies that the instability once again occurs in only the unstable mode.
- For $\triangle t = 0.99 (< 1)$, CNLF is energy stable if $\varepsilon_1 = \varepsilon_2 = 0$; we pick $\varepsilon_1 = \varepsilon_2 = 10^{-4}$ and check for growth in the unstable mode in figure 15. All modes are observed to be stable over a very long time interval.

Test 3: Nonlinear version of Test 2. Consider the 2×2 nonlinear system

$$\frac{du}{dt} + a_1(u) + \varepsilon_1 u - v = 0, \ \frac{dv}{dt} + a_2(v) 10^{-4} v + \varepsilon_2 v + u = 0,$$

$$\text{where } \ a_1(u) = 10^4 |u| u, \text{ and } a_2(v) = 10^{-4} |v| v.$$

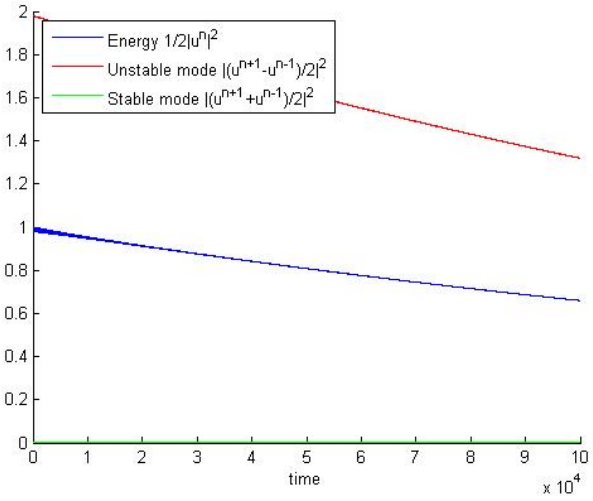

Figure 15: For $\triangle t = .99$ the both unstable and stable modes decay

The matrix Λ is thus

$$\Lambda_{\varepsilon_1,\varepsilon_2} = \begin{bmatrix} \varepsilon_1 & -1 \\ +1 & \varepsilon_2 \end{bmatrix}$$

in which skew symmetry is broken by the small coefficients ε_1 and ε_2. We apply CNLF over a long time interval:

$$\begin{aligned} \frac{u^{n+1}-u^{n-1}}{2\triangle t} + a_1\left(\frac{u^{n+1}+u^{n-1}}{2}\right) + \varepsilon_1 u^n - v^n &= 0, \\ \frac{v^{n+1}-v^{n-1}}{2\triangle t} + a_2\left(\frac{v^{n+1}+v^{n-1}}{2}\right) + \varepsilon_2 v^n + u^n &= 0, \end{aligned}$$

with starting conditions $u^0 = v^0 = u^1 = +1, v^1 = -1$. We calculate $|\Lambda_{0,0}| = 1$ so the two time step condition is $\triangle t < 1$. We observe that:

- For $\triangle t = 1.01 (> 1)$ and $\varepsilon_1 = \varepsilon_2 = 0$ CNLF is unstable; The instability again occurs in only the unstable mode, figure 16.
- For $\triangle t = 0.99 < 1$, CNLF is energy stable (as Step 1 of the proof extends to this nonlinear case) if $\varepsilon = 0$. Pick $\varepsilon_1 = \varepsilon_2 = 10^{-4}$ in this test and find all modes go to zero (figure 17); there is no growth in the unstable mode.

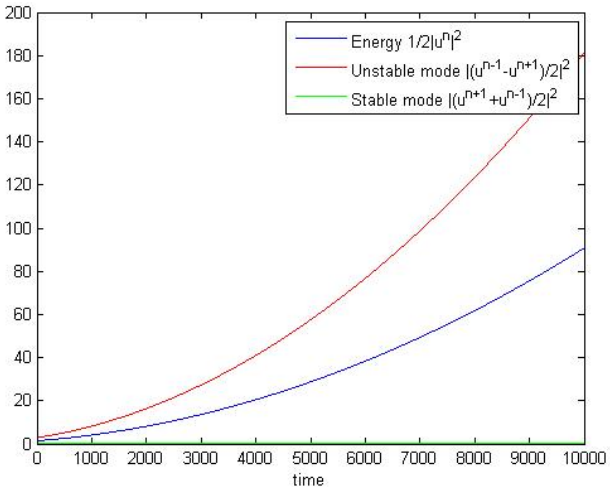

Figure 16: For $\triangle t = 1.01$ the unstable mode grows and the stable mode decays

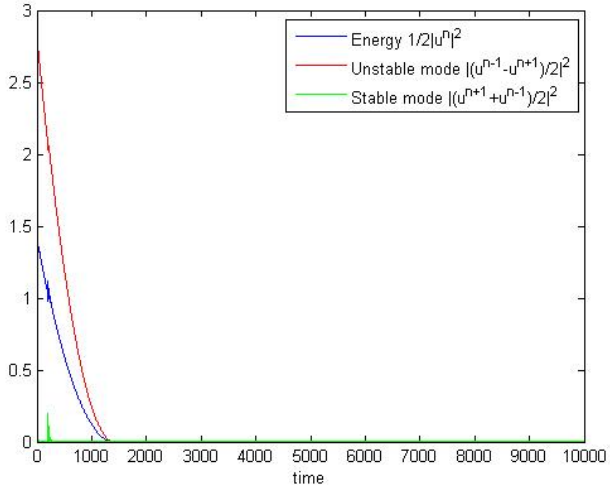

Figure 17: For $\triangle t = 0.99$ both the unstable and the stable mode decay

5.0 CONCLUSIONS

The Crank-Nicolson Leapfrog method with the Robert-Asselin or Robert-Asselin-Williams time filters applied to a linear system is equivalent to a linear multistep method. Under a smaller time step restriction than CNLF alone the multistep method is energy stable and first order accurate with $0 < \nu \leq 1$ and $1/2 < \alpha \leq 1$. The case of $\alpha = 1/2$ increases the accuracy of the multistep method, but it is unconditionally unstable. The multistep method introduces numerical dissipation which controls all modes of CNLF. Stability regions confirm that the multistep method is stable under a smaller time step. Numerical tests show a small increase in the time step restriction derived for the multistep method causes the multistep method to be unstable and a small decrease stable.

The computational mode of Crank-Nicolson Leapfrog method (without a time filter) is stable when applied to a linear system.

BIBLIOGRAPHY

[AKW11] Amezcua, J., Kalnay, E., Williams, P.D.: The effects of the RAW filter on the climatology and forecast skill of the SPEEDY model. Monthly Weather Review **139**(2), 608–619 (2010).
http://dx.doi.org/10.1175/2010MWR3530.1

[ARW95] U. Asher, S. Ruuth and B. Wetton, *Implicit-Explicit methods for time dependent partial differential equations*, SINUM 32(1995) 797-823.

[A72] R.A. Asselin, *Frequency filter for time integration,* Mon. Weather Review 100(1972) 487-490.

[CM10] J. Connors and A. Miloua, *Partitioned time discretization for parallel solution of coupled ODE systems*, BIT Numer. Math. 57(2011) 253-273.

[C80] M. Crouzeix, *Une méthode multipas implicite-explicite pour l'approximation des équationes d'évolution paraboliques*, Numer. Math. 35(1980) 257-276.

[D78] Dahlquist, G.: G-stability is equivalent to A-stability. BIT **18**(4), 384–401 (1978).
http://dx.doi.org/10.1007/BF01932018

[D10] Durran, D.R.: Numerical methods for fluid dynamics: With applications to geophysics, *Texts in Applied Mathematics*, vol. 32, second edn. Springer, New York (2010).
http://dx.doi.org/10.1007/978-1-4419-6412-0

[DC86] Déqué, M., Cariolle, D.: Some destabilizing properties of the Asselin time filter. Monthly Weather Review **114**(5), 880–884 (1986).
http://dx.doi.org/10.1175/1520-0493(1986)114<0880:SDPOTA>2.0.CO;2

[F73] Fornberg, B.: On the instability of leap-frog and Crank-Nicolson approximations of a nonlinear partial differential equation. Math. Comp. **27**, 45–57 (1973)
http://dx.doi.org/10.1090/S0025-5718-1973-0395249-2

[FHV96] J. Frank, W. Hundsdorfer and J. Verwer, *Stability of Implicit-Explicit linear multistep methods*, CWI Report 1996.

[GS98] P.M. Gresho and R.L. Sani, *Incompressible Flow and the Finite Element Method: Advection-Diffusion and Isothermal Laminar Flow*, John Wiley and Sons Ltd, England, 1998.

[JK63] Johansson, O., Kreiss, H.O.: Überdas Verfahren der zentralen Differenzen zur Lösung des Cauchy problems für partielle Differentialgleichungen. Nordisk Tidskr. Informations-Behandling **3**, 97–107 (1963)

[HR07] W. Hundsdorfer and S. Ruuth, *IMEX extensions of linear multistep methods with general monotonicity and boundedness properties*, Journal of Computational Physics 225 (2007) 2016-2042.

[HV03] Hundsdorfer, W., Verwer, J.: Numerical solution of time-dependent advection-diffusion-reaction equations, *Springer Series in Computational Mathematics*, vol. 33. Springer-Verlag, Berlin (2003)

[HW10] Hairer, E., Wanner, G.: Solving ordinary differential equations. II, *Springer Series in Computational Mathematics*, vol. 14. Springer-Verlag, Berlin (2010). http://dx.doi.org/10.1007/978-3-642-05221-7.

[HW80] Haltiner, G., Williams, R.: Numerical prediction and dynamics meteorology. John Wiley & Sons (1980)

[H12] Energy Stability of the Crank-Nicolson Leap-Frog Method with Time Filters. *Technical Report, Department of Mathematics, University of Pittsburgh*, October 2012.

[HLLM13] The Unstable Mode in the Crank-Nicolson Leap-Frog Method is Stable. *Technical Report, Department of Mathematics, University of Pittsburgh*, August 2013.

[HLLT13] Stability Analysis of the Crank-Nicolson-Leap-Frog Method with the Robert-Asselin-Williams Time Filter. *Technical Report, Department of Mathematics, University of Pittsburgh*, January 2013.

[JW11] C. Jablonowski, and D. Williamson, *The pros and cons of diffusion, filters and fixers in atmospheric general circulation models*, pp. 381–493 in: P.H. Lauritzen, C. Jablonowski, M. Taylor, R.D. Nair (eds.) Numerical Techniques for Global Atmospheric Models, Lecture Notes in Computational Science and Engineering, vol. 80, Springer, Berlin 2011.

[JK63] O. Johansson and H.-O. Kreiss, *Über das Verfahren der zentralen differenzen zur Lösung des Cauchy-problems fur partielle Differentialgleichungen*, BIT (Nordisk Tidskr. Informations-Behandling) 3 (1963) 97-107.

[K02] Kalnay, E.: Atmospheric Modeling, Data Assimilation and Predictability. Cambridge University Press (2002). http://dx.doi.org/10.1017/CBO9780511802270

[K03] E. Kalnay, *Atmospheric Modeling, data assimilation and predictability*, Cambridge Univ. Press, Cambridge, 2003.

[K12] M. Kubacki, *Uncoupling Evolutionary Groundwater-Surface Water Flows Using the Crank-Nicolson Leapfrog Method*, NMPDEs, 29 (2012) 1192–1216.

[LT12] W. Layton and C. Trenchea, *Stability of two IMEX methods, CNLF and BDF2-AB2, for uncoupling systems of evolution equations*, ANM 62(2012), 112-120.

[LT14] Li, Y., Trenchea, C.: A higher-order Robert–Asselin type time filter. Journal of Computational Physics **259**, 23–32 (2014). http://dx.doi.org/10.1016/j.jcp.2013.11.022

[L07] Lin, Y.L.: Mesoscale Dynamics. Cambridge University Press (2007). http://dx.doi.org/10.1017/CBO9780511619649

[PX09] Park, S., Xu, L.: Data Assimilation for Atmospheric, Oceanic and Hydrologic Applications. Springer London, Limited (2009).

[R66] Robert, A.J.: The integration of a low order spectral form of the primitive meteorological equations. Journal of the Meteorological Society of Japan **44, Ser. 2**(5), 237–245 (1966)

[R69] A. Robert, *The integration of a spectral model of the atmosphere by the implicit method*, Proc. WMO/IUGG Symposium on NWP, Japan Meteorological Soc. , Tokyo, Japan, pp. 19-24, 1969.

[RL97] A. J. Robert and M. Lepine, *An nomaly in the behavior of a time filter used with the leapfrog scheme in atmospheric models*, Atmosphere-Ocean, 35:sup2, s3-S15, (1997)

[S10] Smith, R.J.: Minimizing time-stepping errors in numerical models of the atmosphere and ocean. Master's thesis, University of Reading (2010)

[TL05] S.J. Thomas and R.D. Loft, *The NCAR spectral element climate dynamic core: Semi-Implicit Eulerian formulation*, J. Scientific Computing, 25(2005) 307-322.

[V80] J.M. Varah, *Stability restrictions on a second order, three level finite difference schemes for parabolic equations,* SINUM 17(1980) 300-309.

[V09] J. Verwer, *Convergence and component splitting for the Crank-Nicolson Leap-Frog integration method*, CWI report 2009, http://ftp.cwi.nl/CWIreports/MAS/MAS-E0902.pdf.

[W09] Williams, P.D.: A Proposed Modification to the Robert-Asselin Time Filter. Monthly Weather Review **137**, 2538–2546 (2009). http://dx.doi.org/10.1175/2009MWR2724.1

[W11] P.D. Williams, *The RAW Filter: An Improvement to the Robert–Asselin Filter in Semi-Implicit Integrations,* Mon. Weather Rev., 139 (2011) 1996–2007.

[W13] Williams, P.D.: Achieving seventh-order amplitude accuracy in leapfrog integrations. Monthly Weather Review, **141**(9), 3037–3051 (2013). http://dx.doi.org/10.1175/MWR-D-12-00303.1